



Exploring the stratospheric/tropospheric response to solar forcing

D. Rind,¹ J. Lean,² J. Lerner,³ P. Lonergan,³ and A. Leboissitier³

Received 12 March 2008; revised 1 August 2008; accepted 20 August 2008; published 16 December 2008.

[1] We use the new Goddard Institute for Space Studies Global Climate Middle Atmosphere Model 3 with four different resolutions to investigate various aspects of solar cycle influence on the troposphere/stratosphere system. Three different configurations of sea surface temperatures are used to help determine whether the tropospheric response is due to forcing from above (UV variations impacting the stratosphere) or below (total solar irradiance changes acting through the surface temperature field). The results show that the stratospheric response is highly repeatable and significant. With the more active sun, the annual residual circulation change features relative increased upwelling in the Southern Hemisphere and downwelling in the Northern Hemisphere. Stratospheric west wind increases extend down into the troposphere, especially during Southern Hemisphere winter, and in some runs the jet stream weakens and moves poleward. The predominant tropospheric response consists of warming in the troposphere, with precipitation decreases south of the equator and in the Northern Hemisphere subtropics and midlatitudes, with increases north of the equator especially over southern Asia. The tropospheric response is often not significant, but is fairly robust among the different simulations. These features, which have been reported in observations and other model studies, appear to be driven both from the stratosphere and the surface; nevertheless, they account for only a small percentage of the total variance. More accurate simulations of the solar cycle stratospheric ozone response, the quasi-biennial oscillation, and coupled atmosphere-ocean dynamics are necessary before any conclusions can be deemed definitive.

Citation: Rind, D., J. Lean, J. Lerner, P. Lonergan, and A. Leboissitier (2008), Exploring the stratospheric/tropospheric response to solar forcing, *J. Geophys. Res.*, 113, D24103, doi:10.1029/2008JD010114.

1. Introduction

[2] The discussion of the influence of solar cycles on the stratosphere/troposphere system has grown increasingly sophisticated in the last decade, owing to a combination of empirical analyses and modeling studies. However, great uncertainty remains concerning the actual tropospheric response, and the potential mechanisms involved.

[3] The troposphere generally appears to warm during solar maximum conditions, although as various studies report, there is disagreement about the details of this warming [e.g., *van Loon and Shea*, 1999, 2000; *Haigh*, 2003; *Gleisner and Thejll*, 2003; *van Loon et al.*, 2004; *Coughlin and Tung*, 2004; *Crooks and Gray*, 2005; *Kodera and Shibata*, 2006]. Magnitudes on the order of a few tenths of a °C, with somewhat higher values in the upper troposphere are reported, seen most clearly during June–August although present on the annual average; there are disagreements as to whether the tropical region warms, or primarily the subtropics through midlatitudes. Precipitation changes

have also been reported, in particular increased precipitation in July and August in the tropical western Pacific, and the various monsoon regions: South Asian, west African, and North American [e.g., *Kodera*, 2004; *van Loon et al.*, 2004, 2007; *Bhattacharya and Narasimha*, 2005; *Kodera and Shibata*, 2006]. The values are not large, generally less than the interannual standard deviation, but in some regions on the order of 15% of the climatology. Additional changes reported involve variations in the Hadley and Ferrel circulations [e.g., *Gleisner and Thejll*, 2003; *van Loon et al.*, 2004; *Haigh et al.*, 2005], with associated changes in zonal winds (i.e., jet stream location).

[4] Somewhat competing theories are proposed to explain tropospheric responses to solar forcing. While probably not mutually exclusive, the various mechanisms have some opposing interpretations and cause-effect relationships. One explanation involves direct forcing of the troposphere associated with total solar irradiance (TSI) heating of the surface. Observations from TSI-observing satellite instruments show a TSI increase from sunspot minimum to maximum of $\sim 0.1\%$, corresponding to a change of about a 0.2 W m^{-2} difference at the ocean surface, which *White et al.* [1997] related to an ocean surface temperature change of some $0.02^\circ\text{--}0.06^\circ\text{K}$ on the decadal scale (compared with an observed value of 0.08°K). An alternative interpretation is that the observed effects are due to atmosphere-ocean interactions producing internal oscillations [*Deser and*

¹NASA Goddard Institute for Space Studies, Columbia University, New York, New York, USA.

²Naval Research Laboratory, Washington, D. C., USA.

³Center for Climate Systems Research, Columbia University, New York, New York, USA.

Blackmon, 1993; Latif and Barnett, 1994], although the fact that the “decadal” oscillation tends to be in phase with the solar cycle seems to be more than just coincidence. White *et al.* [1997] suggested that perhaps the solar forcing influence on the ocean heat budget might in some way excite the natural modes of ocean-atmosphere coupling, or at least cause them to come into phase with it. Meehl *et al.* [2003] reported that in their model increased solar irradiance over land during summer solar maximum conditions helped intensify the monsoon, and more solar radiation over cloud free ocean regions increased evaporation and moisture convergence. van Loon *et al.* [2007] and Camp and Tung [1997] suggested that TSI forcing in the subtropics created temperature gradients and wind conditions that excite an ocean dynamical response, particularly that associated with La Niñas during Northern Hemisphere winter (opposite to what is seen in the annual average observations of White *et al.* [1997]). Note that while the Meehl *et al.* [2003] and van Loon *et al.* [2007] studies both emphasize the importance of TSI increases in the northern subtropics during summer, the former study emphasizes the atmospheric (and land) response, while the latter emphasizes the ocean dynamical response to that heating.

[5] Another theory emphasizes the influence of UV variations in the stratosphere, which is known to respond to solar forcing with warming and increased ozone during solar maximum conditions. In this theory, the latitudinal distribution of UV heating change leads to a relative EP flux divergence that results in a reduction in the Brewer-Dobson circulation. The latter effect, or simply the increased stability in the lower stratosphere, results in less equatorial upwelling in the troposphere, encouraging precipitation off the equator [Kodera and Kuroda, 2002; Kuroda and Kodera, 2002; Kodera and Shibata, 2006]. Crooks and Gray [2005] using the ERA-40 data set found a zonal wind shift consistent with an expansion in the latitudinal extent of the Hadley Cell, the same result that Haigh *et al.* [2005] found as a model response to increased stability in the lower stratosphere (and that same experiment also produced less tropical upwelling, i.e., a weaker Hadley Cell). This is a “top-down” forcing, with the SST response in effect driven from the atmosphere, agreeing with the reduced heat fluxes found by White *et al.* [2003] and the further analysis of White [2006].

[6] Modeling of the solar cycle response has suggested possible influences, but none definitively. Models in general are unable to simulate the necessary stratospheric ozone response, as they produce maximum ozone change in the midstratosphere, instead of in the upper and lower stratosphere as observed [e.g., Shindell *et al.*, 1999; Tourpali *et al.*, 2003; Egorova *et al.*, 2004; Sekiyama *et al.*, 2006]. Some progress is being made in this regard; Austin *et al.* [2006, 2008] included a parameterization for the 27-day solar rotational modulation of ozone photolysis (an effect which peaks during sunspot maximum and therefore has a solar cycle), while varying specified sea surface temperatures and greenhouse gases during the full solar cycle. Although their model still produces an ozone peak at lower altitude than in the observations, it does have a minimum response at 20 mb (and hence a double ozone maximum), an improvement which the authors attribute to using the varying SST and a complete solar cycle [Austin *et al.*,

2006]. Models also produce warming in the stratosphere, although typically less than observed (noting that the actual values are uncertain [Labitze *et al.*, 2002; Tourpali *et al.*, 2003; Egorova *et al.*, 2004]). In the troposphere, modeled temperature responses to solar forcing are typically weak although specifying (unchanging) sea surface temperatures, as in many of these studies, minimizes the response in the lower troposphere. Matthes *et al.* [2004, 2006] did find a solar impact on both the tropospheric and stratospheric meridional circulations, while Shindell *et al.* [2006] concluded that tropospheric ozone changes were an important ingredient in their modeled response.

[7] A number of these issues are explored with new versions of the GISS Global Climate/Middle Atmosphere model 3 [Rind *et al.*, 2007] forced with realistic variations in solar irradiance inputs for the recent past. In particular we attempt to ascertain which if any of the suggested mechanisms is supported by model experiments.

2. Model Experiments

[8] We use the GISS Global Climate Middle Atmosphere Model (GCMAM) [Rind *et al.*, 2007], with an upper boundary at 0.002 mb, and one or more resolutions, in a suite of experiments that we separate into three groups. In all experiments the models are forced with a time series of monthly values of the Sun’s spectral irradiance (Figure 1) binned onto 190 wavelength bands. The integrated spectrum matches the total irradiance, and the longer-term changes are consistent with trends in magnetic flux simulated by the Naval Research Laboratory flux transport model since 1713 [Wang *et al.*, 2005; Lean *et al.*, 2005]; for the period of our simulations, from 1950 through 2004, long-term irradiance trends are minimal.

[9] The GISS model handles shortwave radiation differently depending upon the spectral interval. In the UV (short of 0.33 microns), ozone is highly absorbing, and so the bands are handled via an analytic path length formulation integrating solar spectral and ozone variations [Lacis and Hansen, 1974]. In the visible and near-IR there are two broadband channels (0.33–0.77 microns, and 0.77 to 0.86 microns). At wavelengths longer than 0.86 microns, there are 16 pseudospectral correlated-k distribution intervals, which are not spectrally contiguous [Hansen *et al.*, 1983].

[10] Most of the experiments use the LINOZ scheme for ozone photochemistry in the stratosphere [McLinden *et al.*, 2000] with an online photochemistry tracer [Rind *et al.*, 2002]. In the troposphere, ozone is calculated using monthly mean ozone production and loss rates archived from GEOS-CHEM, a global photochemical transport model [Bey *et al.*, 2001; Park *et al.*, 2004; see also Rind *et al.*, 2007]. In discussing the ozone calculations subsequently, we refer to both the stratosphere and troposphere ozone chemistry calculations simply as the “LINOZ scheme.”

[11] The experiments were grouped according to three different implementations of sea surface temperatures (SST): calculated SST; varying values based on the historical record; and constant values specified from the climatological average. The SST were calculated via a mixed layer model with heat diffusion through the bottom, and specified ocean heat transports, i.e., a “q-flux” model. The calculated

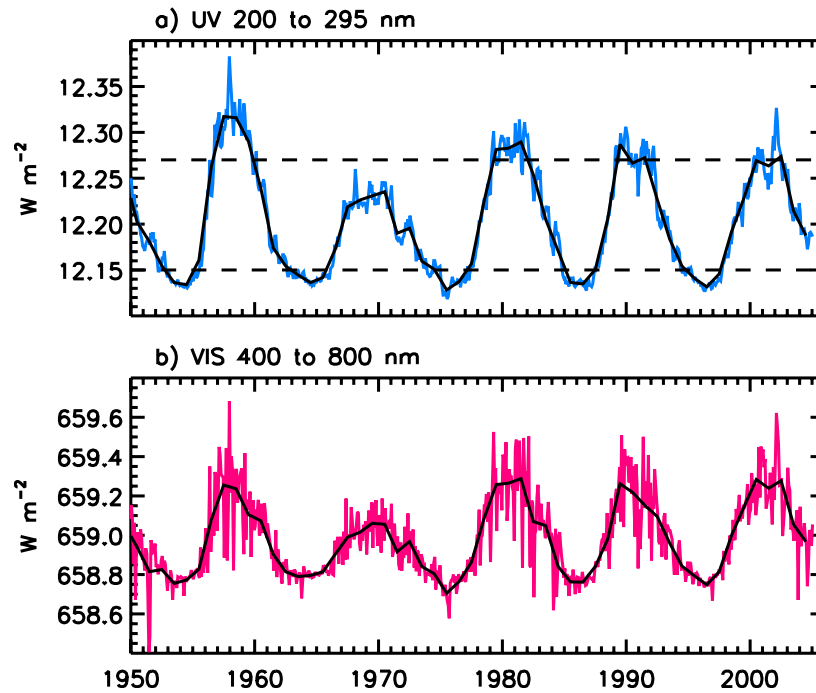


Figure 1. Monthly (and annual) values of incident (a) UV (200–295 nm) and (b) visible (400–800 nm) radiation used in these experiments. Values above and below the dashed lines define the years used for solar maximum and solar minimum conditions, respectively.

SST experiments explicitly allow for a solar cycle influence on the upper ocean while the experiments with historical SST implicitly incorporate any such influence [e.g., *White et al.*, 1997]. The climatological SST test the model response when no such influence is allowed. Control runs (with unchanged solar radiation) were run for each SST configuration to obtain standard deviations for assessing the significance of the changes.

[12] Since we do not use a fully coupled atmosphere-ocean model in these experiments, we cannot directly test the hypothesis that climate may respond to solar forcing via La Niña-type pattern generation. It is in any event doubtful that the ability of current models to generate ENSO is adequate for performing such an assessment, a conclusion also reached by *Intergovernmental Panel on Climate Change* [2007] for the much greater forcing associated with green-

house warming. To the extent that the Q-flux approach reproduces some of the observed solar relationships it automatically implies that changes in ENSO state are not necessary for the occurrence of the described solar effects.

[13] Table 1 lists the experiments performed in the first group, with the model using calculated, hence varying, SST (“V”). The first experiment (“S-V”) (with the 4×5 , 23 layer model, henceforth M23) varied the input solar spectral irradiance and allowed the model to respond, its purpose being to test solar forcing directly, without any stratospheric ozone feedback. The second experiment (also done with M23 version of the model) allowed “dynamic” ozone feedback, in that any change in ozone induced by altered circulation in the stratosphere affects the model’s atmospheric radiation (“SOd-V”). In the third set of experiments, the LINOZ photochemistry was enabled so that

Table 1. Model Experiments With Calculated SST^a

Name	Resolution	SST	Forcing	Ozone
S-V	M23	varying	solar	climatological
SOd-V	M23	varying	solar	varying only owing to advection, not owing to photochemistry
SO-V (STANDARD)	M23 (1 run)	varying	solar	varying from LINOZ
SV-V	M53 (3 runs)	varying	solar, volcanic aerosols	varying from LINOZ
SA-V	M53	varying	solar, GHG, trop aerosols, volc aerosols, trop ozone	varying from LINOZ

^aAll experiments were run for the years 1950–2005. Model resolutions: 4×5 , 23 layers (M23); 4×5 , 53 layers (M53); 2×2.5 , 53 layers (F53); 2×2.5 , 102 layers (F102).

Table 2. Model Experiments With Historical SST (1950–2005)

Name	Resolution	SST	Forcing	Ozone
S-H	M53	historical	solar	climatological
SO-H (STANDARD)	M23, M53, F53, F102	historical	solar	varying from LINOZ
SA-H	M23, M53, F53, F102	historical	solar, GHG, trop aerosols, volc aerosols, trop ozone	LINOZ 30–58 km varying from observations 10–30 km
SOs-H	M53	historical	solar	solar cycle variation from SAGE II observations

ozone changes occurred owing to the altered UV radiation associated with the solar cycle (“SO-V”) (in addition to any dynamically induced changes). Both M23 and M53 (i.e., 4×5 , 53 layer) models were used for these simulations, with the M53 version run 3 times, starting from slightly different initial conditions. Since the 9-year difference between the El Chichon and Pinatubo eruptions has been a confusing factor when assessing the 11-year solar influence, the fourth experiment (SV-V) tested the influence of observed volcanic aerosol perturbations on solar forcing, by including them for this time period, together with LINOZ calculated ozone in M53. The fifth experiment combined volcanic forcing and additional anthropogenic forcing changes: trace gases (e.g., CO₂, methane, N₂O, CFCs, etc.), tropospheric aerosols and tropospheric ozone changes (“SA-V”), with M53. These forcings are specified by Hansen *et al.* [2007].

[14] The second group of experiments, listed in Table 2, used historical SST (“H”) based on data from Rayner *et al.* [2003], Reynolds and Smith [1994] and Smith and Reynolds [2004]. The first experiment, with the M53 model, used variable solar radiation with historical SST and climatological ozone (“S-H”). The second experiment allowed ozone to respond via the LINOZ scheme (“SO-H”), repeated for four different resolution models: M23, M53, F53 and F102, the latter two having $2^\circ \times 2.5^\circ$ horizontal resolution, with the indicated number of vertical levels. In this and the other experiments, the purpose of using different vertical and horizontal resolution was to test the degree to which the solar influence in models is resolution dependent. The third experiment (“SA-H”) used all the climatological forcings (as in SA-V) except with observed ozone changes below 30 km (so as to include the ozone hole), while still allowing

calculated LINOZ ozone from 30 to 58 km. This configuration was also run with all four resolution models. To assess the importance of the exact shape and magnitude of the ozone variation, the fourth experiment utilized the SAGE ozone observations (“SOs-H”). This was implemented by adding climatological ozone deviations for solar maximum and solar minimum conditions for the appropriate years, determined relative to the averages of SAGE ozone during the 20-year average record. The SAGE ozone maximum minus minimum values have been discussed by Soukharev and Hood [2006] and Randel and Wu [2007], and are shown in the next section. The screened version of the data set used is from Rind *et al.* [2005].

[15] The third group of experiments, Table 3, repeated several simulations of the second group, but with climatological average (i.e., invariant) SST (“C”) (derived for the same 1950–2005 time period). The first set of experiments used solar forcing with the LINOZ ozone photochemistry (“SO-C”) in the M23, M53, F53 and F102 models. The second experiment used instead the SAGE ozone solar maximum and solar minimum ozone perturbations (“SOs-C”) in the M53 model. The third set of experiments was similar to the first, but with the inclusion of all the other forcings (“SA-C”) and was again run in all four models. The fourth and fifth experiments used the LINOZ photochemistry with added forcing to produce the east and west QBO winds, as in work by Balachandran and Rind [1995], extended up to 1 mb following the suggestion of Matthes *et al.* [2004] (“SO-E-C, ”“ SO-W-C”), in the 4×5 , 53 layer version.

[16] Each of the experiments in Tables 1, 2 and 3 was run for 55 years (1950 to 2004). Of a total of 29 separate

Table 3. Model Experiments With Climatological Average SST (1950–2005)

Name	Resolution	SST	Forcing	Ozone
SO-C (STANDARD)	M23, M53, F53, F102	climatological	solar	varying from LINOZ
SOs-C	M53	climatological	solar	solar cycle variation from SAGE II observations
SA-C	M23, M53, F53, F102	climatological	solar, GHG, trop aerosols, volc aerosols, trop ozone	LINOZ 30–58 km varying from observations 10–30 km
SO-E-C	M53	climatological	solar, relaxing to QBO east winds	varying from LINOZ
SO-W-C	M53	climatological	solar, relaxing to QBO west winds	varying from LINOZ

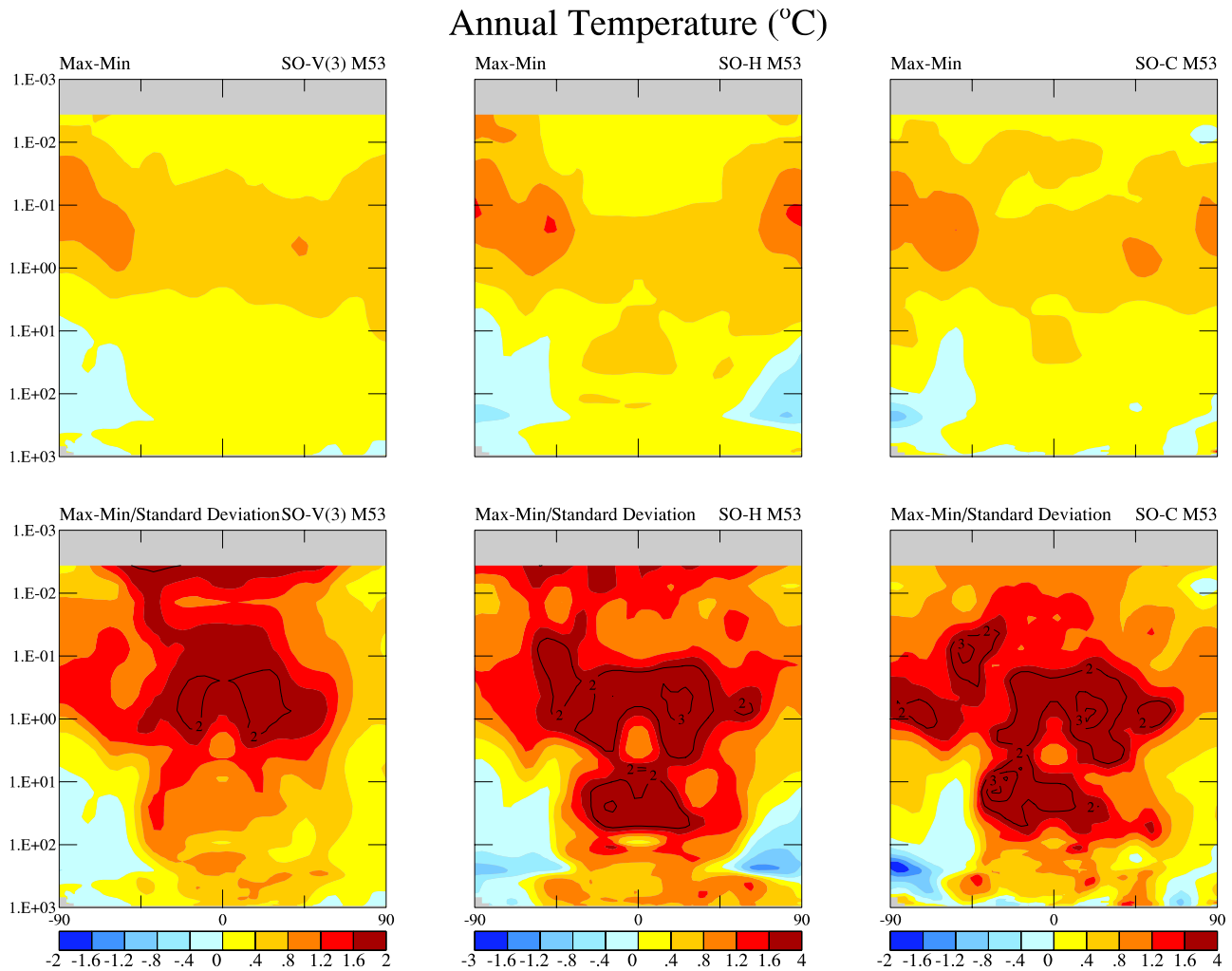


Figure 2a. (top) Annual temperature change between solar maximum and solar minimum conditions in the model simulations. (left) Results are shown for the simulations with (calculated) varying SST, (middle) historical SST for the 1950–2004 time period, and (right) climatological-average SST for the same time period. (bottom) Annual temperature changes divided by the standard deviations from respective control runs (with unchanging solar radiation) for the three SST approaches. Note the color table is used for both rows, representing (top) $^{\circ}\text{C}$ and (bottom) relative standard deviations.

simulations, amounting to about 1600 simulated years with solar forcing, 26 experiments included calculated or observed ozone changes. While the experiment runs were time-varying over approximately five solar cycles, some results are presented as changes between solar maximum and solar minimum conditions (for comparison with observations and other modeling results). As shown in Figure 1, years “qualified” as solar maximum or minimum by the level of solar UV irradiance in the wavelength band from 200 to 295 nm. Designated solar maximum years were those in which the integrated UV irradiance in this spectral interval exceeded 12.27 W m^{-2} , while for solar minimum the values were less than 12.15 W m^{-2} , with 12 years in each category. Overall, the annual difference in total incident solar radiation between solar maximum and minimum at the top of the atmosphere equaled $\sim 0.2 \text{ W m}^{-2}$.

[17] Also evident in Figure 1, with the set of years used here, solar maximum conditions follow (come later than) solar minimum values. Given that the troposphere has been

warming over the past several decades, and that atmospheric CO_2 has been increasing (which affects stratospheric temperatures as well), there is an “anthropogenic” influence in the solar maximum minus solar minimum calculation, as the maxima are continually associated with higher CO_2 levels than the minima. To examine the effect of this bias, we occasionally create an ‘altered’ maximum minus min, dropping the first minimum and the last maximum (which now means the minima are associated with increased CO_2). We show in section 3.6 that this does make a difference in some of the temperature fields. Finally, to highlight some features we also show full solar cycle correlations with the input UV field (e.g., Figure 1).

3. Results

[18] We formulate our results as responses to eight questions. Results from the standard runs (labeled STANDARD in Tables 1–3) are presented first, with additional runs

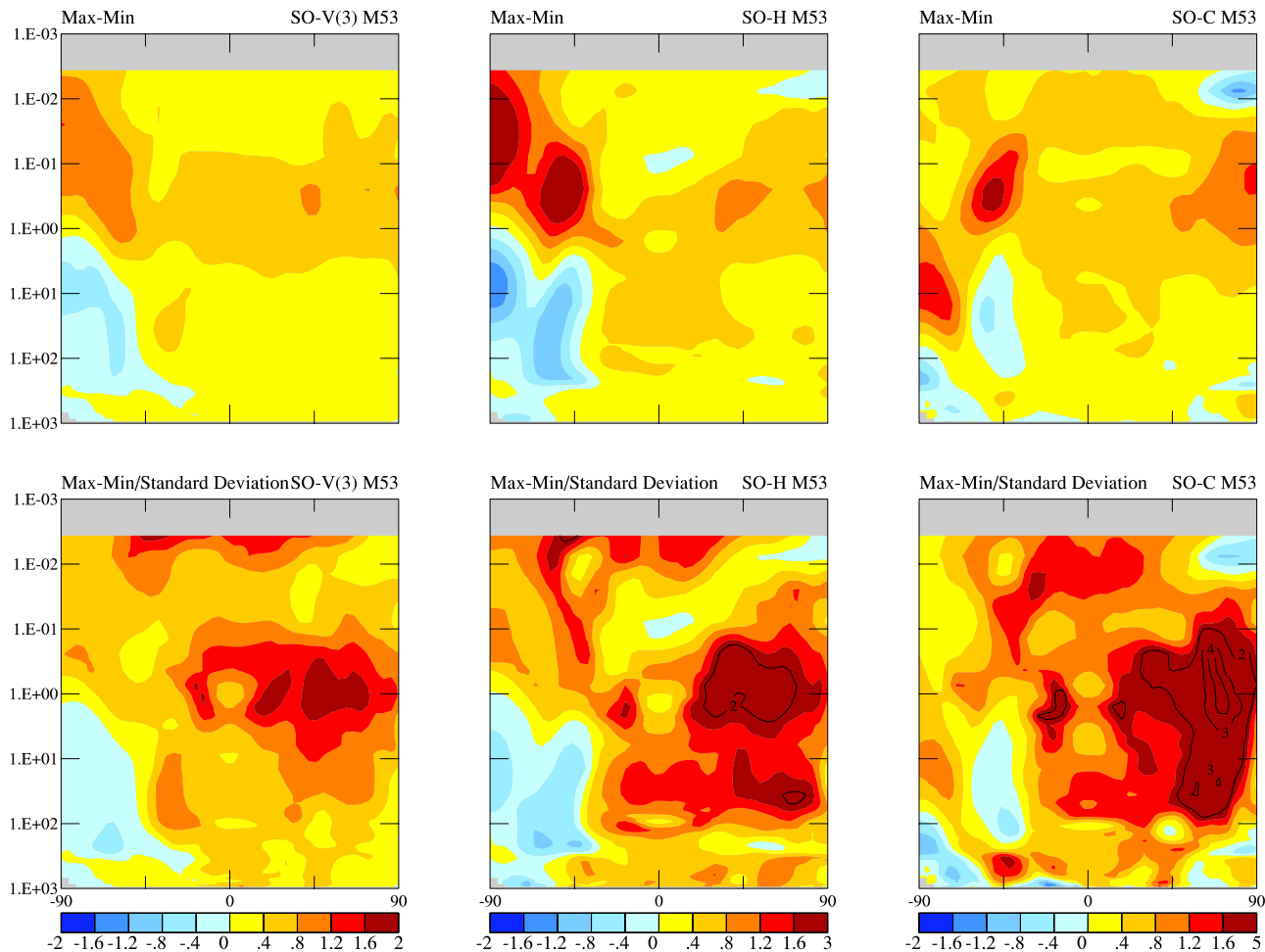
June-July-Aug Temperature ($^{\circ}\text{C}$)

Figure 2b. As in Figure 2a except for the June–August time period.

incorporated to address the various questions. We identify the standard experiments as those which include the necessary physical processes, incorporating varying solar spectral irradiance and utilizing the LINOZ ozone calculation, combined with the different treatments of the ocean. In general, the averaged results for the three SO-V simulations are shown together.

3.1. Do the Standard Runs Reproduce the Observed Stratospheric and Tropospheric Temperature Changes?

[19] Shown in Figure 2a are the annual average temperature changes between solar maximum and solar minimum conditions (as defined above and in Figure 1) from the standard experiments with the 53-layer model (M53) for the years 1950–2005. The actual differences are shown in Figure 2a (top), and the values normalized by the respective control run interannual standard deviations are given in Figure 2a (bottom). Using a standard “Students” t test, only the values in the last color categories (of Figure 2a, bottom) are significant at the 95% level. Many of the reported tropospheric effects are of marginal significance, which is why we show (in effect) the full range of significance results here.

[20] The stratospheric temperature responses indicate peak tropical warming of about 0.7°C . Although highly significant, this warming is smaller than the 1K determined from NCEP reanalysis data, and a factor of 2 or more smaller than the $1.5^{\circ}\text{--}2^{\circ}\text{C}$ values derived from rocketsonde data, but it is in agreement with the magnitude derived from analysis of SSU data by *Scaife et al.* [2000] (see the discussion by *Hood* [2004]). A further discussion of the controversial temperature signal in this region is included in section 4.1. The stratospheric response is relatively independent of how sea surface temperatures are determined.

[21] In the June–August time frame, shown in Figure 2b, warming similar to that in the annual average occurs in the stratosphere, although now all three models also show more cooling at Southern Hemisphere upper midlatitudes in the low stratosphere to midstratosphere, in agreement with NCEP reanalysis observations [e.g., *van Loon and Shea*, 2000].

[22] Tropospheric tropical warming occurs in all simulations, although from a quantitative standpoint, the results are not significant. The magnitudes, generally on the order 0.2°C , are about half that derived from NCEP reanalysis [*van Loon and Shea*, 2000]. While use of the climatological

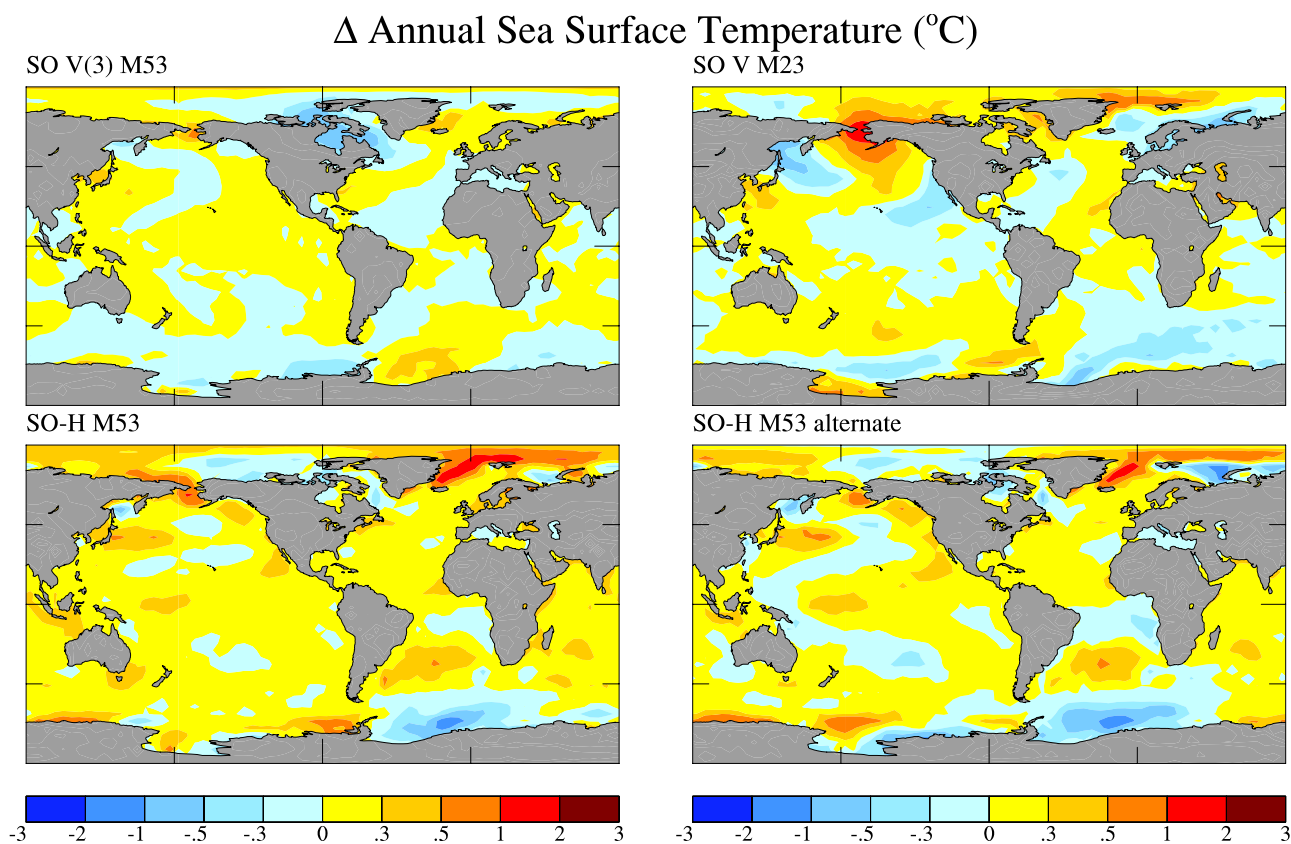


Figure 3. Sea surface temperature changes between solar maximum and solar minimum conditions. (top) Results from the runs with calculated SST, for (left) the three run ensemble in M53 and (right) the single simulation in M23. (bottom left) Results for the historical SST changes. (bottom right) As an alternate, results are also given when the last solar maximum and first solar minimum are removed.

SST (in SO-C) undoubtedly limits the tropospheric response, the values are not much larger with the calculated SST. Nor would they be much different with a full dynamic ocean, whose response time would be much longer than the time difference between solar maximum and minimum years, except for possible ENSO-type response; simple inclusion of a deep ocean with heat diffusion through the bottom of the mixed layer also makes little difference on this timescale, although it would affect the magnitude of overall trends during the 50-year time period. The run with calculated SST actually has somewhat lower significance in the upper troposphere and lower stratosphere compared with the other simulations. When the historical SST are used, warming approaches 0.4°C , and is $> 90\%$ significant in some upper tropospheric regions. (We show below that the correlation of temperature with the solar cycle is often significant in the troposphere.)

3.2. Do the Δ SST in the Calculated Ocean Runs Match Those in the Historical Data?

[23] Shown in Figure 3 are the annual changes between solar maximum and solar minimum years simulated using calculated SST (Figure 3, top) and historical SST (Figure 3, bottom). Calculated results are shown for both the 53 (Figure 3, left) and 23 (Figure 3, right) layer models, respectively. The patterns are not coincident but they all show warming in the North Pacific off of Asia (again, using

a full dynamic ocean would not alter this conclusion, unless ENSOs were generated by this small forcing, a result probably beyond the ability of coupled atmosphere-ocean models to produce with confidence). There is greater widespread warming between solar maximum and minimum conditions with the historical SST (Figure 3, bottom left), which enhances the tropospheric response in Figure 2a. Its pattern is consistent with that determined by *White et al.* [1997] from observations, which is not surprising since the same observations are used to create the historical SST data set. Both the historical and calculated SST changes show that during June–August there is somewhat greater warming north of the equator (evident in the annual picture as warming off the coast of Asia) which as discussed below influences precipitation.

3.3. Do the Standard Runs Produce the Observed Ozone Difference, and if Not, What Difference Does It Make?

[24] In all of the standard runs ozone is calculated with the LINOZ photochemical scheme. Shown in Figure 4a are annual changes in temperature (Figure 4a, left), shortwave radiative heating (Figure 4a, middle) and ozone (Figure 4a, right) between solar maximum and solar minimum conditions in M53. The corresponding ozone profile change is similar to that determined by other GCMs [e.g., *Austin et al.*, 2006], with peak ozone change of close to 2% in the

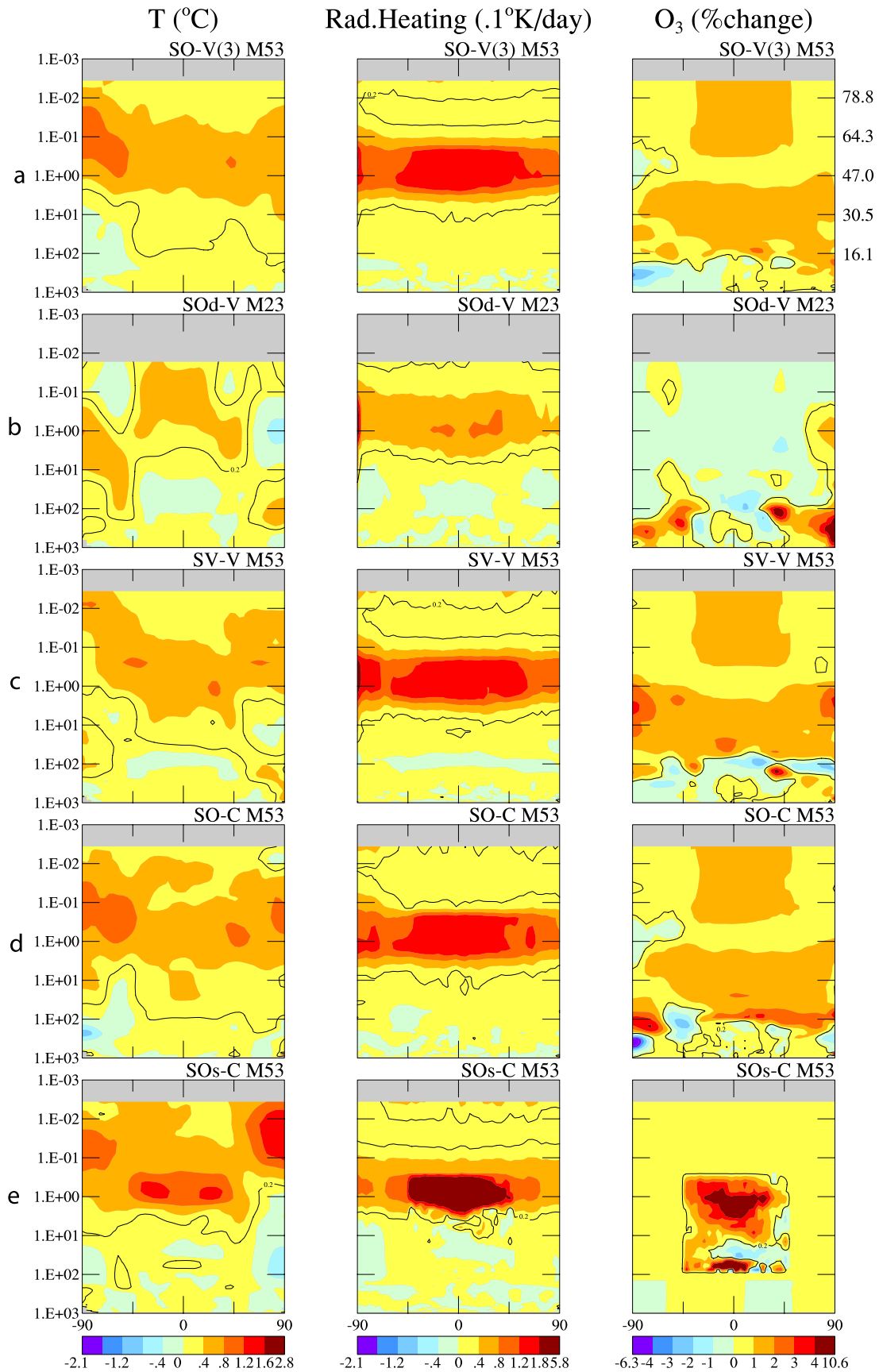


Figure 4

midstratosphere, not in the upper stratosphere as suggested by observations [e.g., *Soukharev and Hood, 2006*]. The results also show a maximum in the lower stratosphere (most clearly visible in SO-C) of around 2%, seen in some observations [e.g., *Soukharev and Hood, 2006*]; *Marsh and Garcia [2007]* suggest that it is influenced by ENSO events, rather than just the solar forcing, but that's clearly not the case with the climatological average SST in SO-C. Note also that the results generally show ozone increases in the troposphere, although not everywhere.

[25] The Figure 4b shows a similar experiment except that ozone photochemistry is invariant to the change in solar UV radiation (ozone changes only via altered dynamics). In this case, the radiative heating rate change is reduced by about half, the temperature change is accordingly smaller and there is minimal change in stratospheric ozone. So allowing the ozone to respond photochemically to altered UV radiation is essential for the model's ability to simulate the solar-forced response in the stratosphere, a result found by many other researchers [e.g., *Shindell et al., 2006*]. (Note that the results shown for this experiment are from M23, while the STANDARD experiment (Figure 4a) is for M53; however, the M23 and M53 simulations of the STANDARD experiment are quite similar.) Interestingly, this run did show ozone increases in the extratropical lower stratosphere of both hemispheres, associated with altered dynamical transports (since there was no photochemical response), although not in the tropical lower stratosphere as observed [*Soukharev and Hood, 2006*].

[26] The equivalent results for the STANDARD experiment with climatological SST are given Figure 4d, with very similar changes between solar maximum and solar minimum conditions as with the calculated SST. (Results from Figure 4c, associated with volcanic aerosol changes, are discussed in section 3.6.)

[27] The ozone changes employed by using solar maximum and minimum values observed from SAGE II (instead of LINOZ) are shown in Figure 4e (right). Changes were incorporated only from 45°N to 45°S, as the changes in the polar regions were quite inconsistent from different maximum to minimum conditions, and were probably influenced by highly variable dynamics. The SAGE II instrument does indeed show ozone differences peaking in the upper stratosphere, not midstratosphere. In addition, the magnitudes are bigger than the model calculated, with a peak change close to 4%; as shown by *Soukharev and Hood [2006]* [see also *Stratospheric Processes and their Role in Climate, 1998*], this is also about double the value determined from SBUV and UARS HALOE measurements. The shortwave radiative heating difference (Figure 4, middle) is correspondingly amplified, and the stratospheric temperature response (Figure 4, left) is also somewhat greater, with values exceeding 1°C.

[28] The SAGE II ozone profile change also indicates a maximum response to the solar cycle in the lower stratosphere and minimum response in the midstratosphere fea-

tures that have been linked to dynamical responses affecting the troposphere. The temperature response (Figure 4e) likewise shows a minimum in the midstratosphere; the change relative to the simulation with the LINOZ profile and climatological SST (Figure 4d) is about -0.6°C , or more than 2 standard deviations. The equivalent experiment with historical SST (SOs-H, not shown) gives a very similar result, increasing confidence in its robustness. It is consistent with the radiation response (Figure 4, middle), without a strong dynamical influence. But even with the ozone solar cycle specified by the SAGE II observations, the model simulations show only a slight temperature change in the lower stratosphere, the effect differing only marginally from that generated in the lower stratosphere with invariant ozone (Figure 4b). (Note that dynamical changes resulting from the SAGE II ozone were allowed to influence the temperature structure throughout.) Tropospheric temperature changes show little impact. Using climatological SST may diminish the tropospheric differences, but there is little response even in the upper troposphere, where dynamical changes are expected to have an influence. Again, the same experiment but with historical SST (not shown), likewise showed little apparent tropospheric impact relative to the historical SST simulation with LINOZ calculated ozone.

3.4. Does Model Resolution Make a Difference?

[29] It is supposed that finer resolution models may produce a stronger tropospheric response via a more complete interaction with the stratosphere, but we find no evidence of this in our simulations. Figures 5a–5c compares the results from experiments made with four different resolution models (2×2.5 and 4×5 with 23, 53 and 102 layers, using historical SST). Figure 5a (with historical SST) shows the correlations at different latitudes and heights of the simulated ozone densities with the UV irradiance (Figure 1), as determined from the five complete solar cycles of the model runs. Given that the different resolution models have somewhat different dynamical properties [*Rind et al., 2007*], the correlation patterns do differ in some details, but each shows the same general characteristics: high correlations of ozone and solar UV radiation above the stratopause, minimum correlation (though still positive) around 50 km, and greater correlation in the midstratosphere. The solar cycle–ozone correlations for the calculated and climatological SST (not shown) also have little distinction among the resolutions, and are quite similar to those with the historical runs. The solar cycle–temperature correlations with historical SST (Figure 5b) likewise have great similarity among the different resolution models, including maximum correlation in the subtropical lower stratosphere, a feature that has been observed [e.g., *Crooks and Gray, 2005*] with ERA reanalysis data but it does not appear in SSU/MSU data [*Keckhut et al., 2005*]. However, the negative correlation in the tropical lower stratosphere with three of these four resolutions

Figure 4. Annual average solar maximum minus solar minimum change in (left) temperature, (middle) solar radiative heating rate, and (right) ozone for different simulations. Results with calculated SST (a) for the STANDARD run, (b) when ozone is altered only by solar-induced dynamical changes, and (c) when the history of volcanic aerosols is used as well. Results with climatological SST (d) for the STANDARD run and (e) when SAGE II ozone values were used to generate solar maximum and minimum conditions. (A representative height scale is shown top right.)

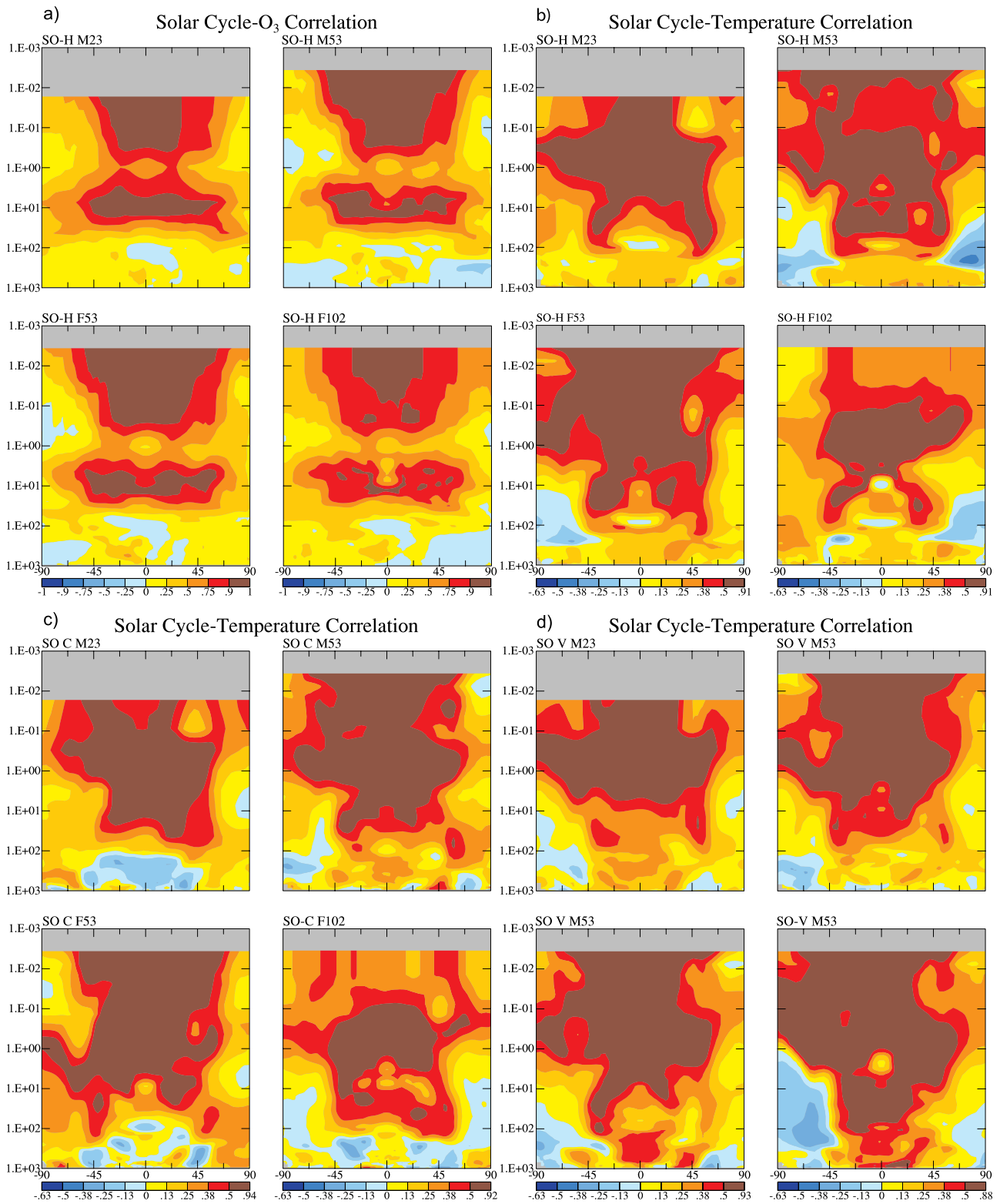


Figure 5. Annual correlations between varying solar UV irradiance (200–295 nm) and model responses with different resolution for (a) ozone with historical SST, (b) temperature with historical SST, and (c) temperature with climatological average SST. (d) The correlation with calculated SST for model M23 and each of the M53 runs separately.

(and a minimum in the other) is similar to that shown by *Keckhut et al.* [2005] with SSU/MSU data, and is also present to a much lesser degree in the ERA reanalysis [*Crooks and Gray, 2005*]. The stratospheric correlations with the varying UV for both ozone and temperature are highly significant.

[30] In the troposphere the correlation of solar UV radiation with temperature (Figure 5b) is significant at the 95% level (and even higher in some locations), and is in good agreement with observations from reanalysis data [*Labitzke et al., 2002*]), including the minimum in correlation near the tropical tropopause in the ERA-40 data set [*Crooks and Gray, 2005*] (true in the model for ozone as well). However, these results are for the simulations with historical SST, which of course is how reanalysis data are generated. We repeated these correlations with the other two standard experiments, and the results are shown in Figures 5c and 5d. With climatological SST (Figure 5c), the tropospheric correlation is often muted or nonexistent; preventing the SST from changing is expected to limit the tropospheric response. The response for M53 in the troposphere appears greater than in the other resolutions; this is not due to a greater ozone response (there is not), nor to a dynamic response of greater subsidence, or even greater tropical precipitation compared with the other resolutions (as shown later, neither of those things occur). Caution is necessary when considering changes of this nature, as is emphasized by the results in Figure 5d. In these runs with calculated SST, we show the three individual simulations with M53, as well as M23 to illustrate the inherent variability. Here the solar forcing acts directly on the ocean temperatures and in the correlation patterns of these runs, the tropospheric response is generally significant, in some cases highly so (>99%), but there is strong variability from run to run, now even with the same model. Negative correlations tend to occur at higher latitudes. Negative/minimum correlations in the tropical lower stratosphere/upper troposphere occur more frequently in the runs with historical SST, lending some credence to the idea that it is a product of influence inherent in the SST data set, including possibly ENSOs [*Marsh and Garcia, 2007*].

3.5. Is the Solar Cycle Effect Greater With the East QBO?

[31] *Labitzke* [2004] found in the NCEP/NCAR reanalysis data a stronger solar cycle response in Northern Hemisphere summer during the east phase of the QBO. To test this response, we forced the model to have a QBO by relaxing the tropical winds back to either east or west, and running the 55 year simulations with climatological SST. The *Labitzke* [2004] study focused on July (to avoid the dynamic influences of Northern Hemisphere winter), and considered both correlations of temperature with 10.7 cm solar flux data (a proxy for UV variations), as well as solar maximum minus minimum temperatures. When we compared the maximum minus minimum temperatures, the results were dependent upon whether we used values defined by the UV, or just the maximum and minimum for each cycle. Therefore we focus on the correlations, and use the full season (June–August).

[32] Shown in Figure 6a is the correlation of UV with temperature in the East phase (Figure 6, left) and the west

phase (Figure 6, right). Consistent with *Labitzke's* analysis, the region of significant correlation is considerably broader, and extends to lower altitudes in the east phase; the resulting magnitudes, and even the appearance of the east phase correlation, is similar to that shown by *Labitzke* [2004] (including the region of negative correlation at high southern latitudes, but not the large positive correlation in the tropical lower stratosphere). The west phase significant correlation is much more restricted, as it was in the *Labitzke* results, although it is somewhat broader than in the NCEP/NCAR observations. Whether June–August averages would provide higher correlations in the observations is unknown; it did in the model. In neither case is there much difference in the tropospheric response, although again the use of climatological SST dampens such effects.

[33] In both the model and observations, the greatest correlations with the solar cycle during this season are in the Northern (summer) hemisphere. To understand how this is happening, and the difference between the two QBO phases, we show in Figures 6b, 6c, and 6d the correlations between the varying UV and the zonal winds, the northward EP flux and the vertical EP flux. In both QBO phases higher UV is associated with greater upward flux of wave energy from the extratropical Southern Hemisphere (winter) troposphere, although more so in the east phase (Figure 6d). The increased vertical flux is associated with small increases in tropospheric eddy kinetic energy at upper midlatitudes, on the order of 2% (East QBO) and less than 1% (West QBO); however, the effect in the stratosphere is much larger, with eddy kinetic energy changes peaking at close to 20% around 65°S and 10 mb in both phases. With the east QBO, the vertical flux in the Southern Hemisphere then goes northward in the low stratosphere to midstratosphere, across the equator to the Northern Hemisphere extratropics (Figure 6c, left), and then goes upward again (Figure 6d, left), where it produces eddy kinetic energy increases of about 10% in the (now) summer hemisphere. The vertical fluxes and added eddy energy in the Northern Hemisphere are associated with equatorward heat transports (it is warmer at the pole in this season) that help warm the Northern stratosphere at midlatitudes; note that the vertical flux in the Northern stratosphere is not coming directly from the troposphere below, but by this circuitous route from the Southern (winter) troposphere where eddy energy is more prevalent in this season. In the case of the west QBO, not only is the vertical EP flux weaker (Figure 6d, right), but its northward movement across the equator is much weaker (Figure 6c, right), as is then the subsequent upward flux in the Northern extratropics, and the associated equatorward heat transport. Hence the correlation with temperature is less extensive. But with wave energy flux not crossing the equator in the west phase, a higher correlation with warming occurs in the lower tropical stratosphere, which acts to increase the Southern Hemisphere latitudinal temperature gradient. This then helps the upper stratospheric zonal wind increase to extend down to lower levels in the west phase than in the east phase, and through feedback mechanisms discussed by *Kuroda and Kodera* [2002], into the troposphere.

[34] Of course, the QBO here is being forced, not resulting from model processes, and in addition, it is not time- and altitude-varying, all aspects that could make a

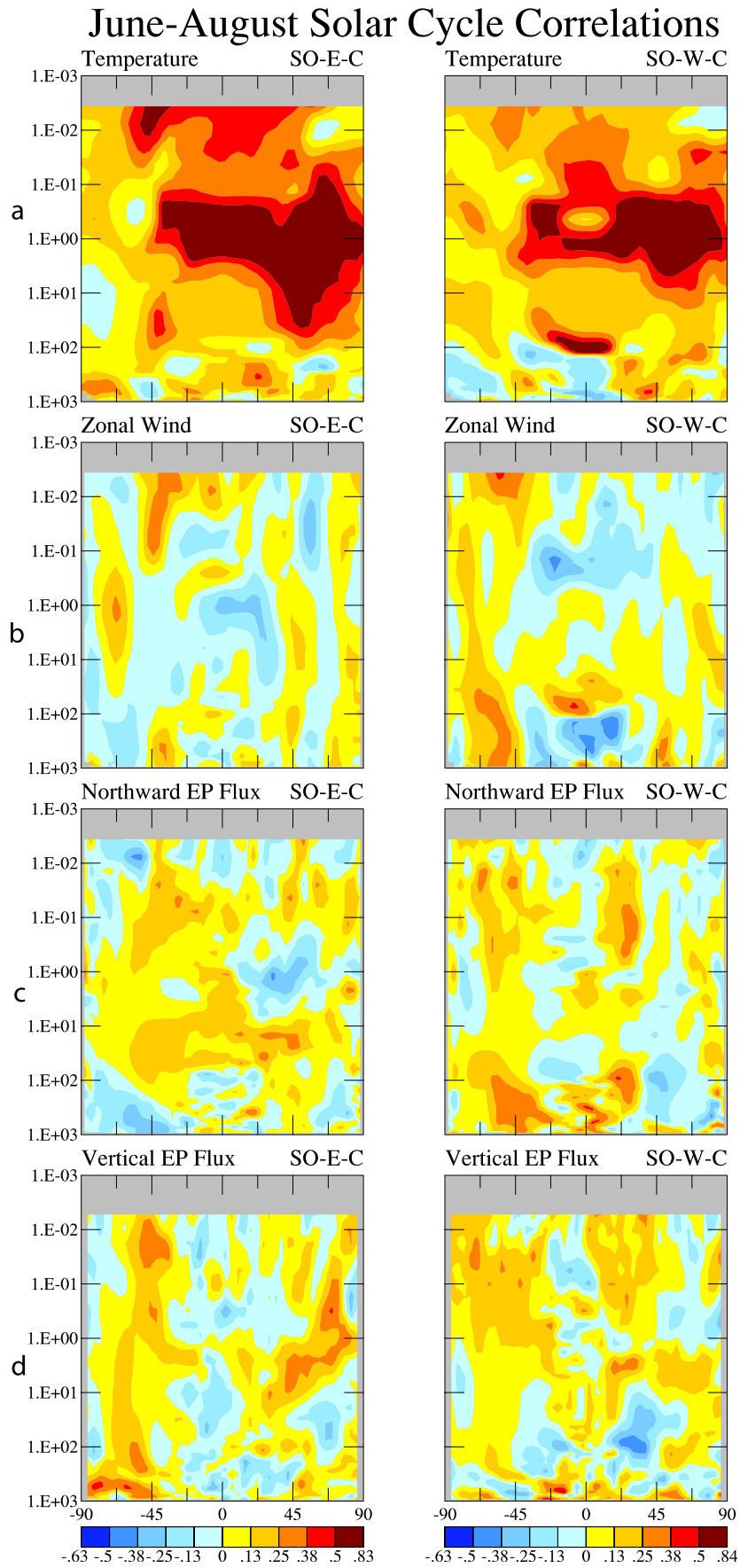


Figure 6

difference. The results for December–February provide a test of the verisimilitude of the model’s QBO/solar cycle interaction, at least within the context of the extratropical response to solar-maximum minus solar-minimum conditions. Presented in Figure 7 are the temperature, zonal wind and 10 mb height differences between solar maximum and solar minimum conditions for the east (Figure 7, left) and west (Figure 7, right) QBO, as well as the difference in vertical EP fluxes. Consistent with simulations with earlier versions of the model [Balachandran and Rind, 1995; Balachandran et al., 1999], the different phases result in diametrically opposite solar cycle impacts, with a stronger polar vortex during solar maximum in the east phase, and a weaker polar vortex during solar maximum in the west phase, in agreement with observations [e.g., Labitzke, 1987]. The differences for December–February (as opposed to June–August) relate to the vertical EP flux directly below from the troposphere (affected by propagation differences), which are reduced (increased) in the QBO east (west) phase; hence so is the poleward heat transport, producing a colder (warmer) lower stratosphere, increased (decreased) extratropical west winds and a stronger (weaker) polar vortex. These effects obviously extend down into the troposphere [see also Rind and Balachandran, 1995]. So for both seasons the use of the forced QBO has not kept the model from reproducing some aspects of the solar/QBO relationships seen in observations.

3.6. Do the Other Forcings Make a Difference?

[35] Solar cycle effects during the 20th century occur simultaneously with the effects of other forcings, such as increasing concentrations of anthropogenic gases and changes in volcanic aerosols. Proper isolation of the solar signal by removing these other effects from the observations is a difficult procedure with many associated uncertainties. For example, is linear trend analysis the proper way to remove anthropogenic influences, some of which could certainly be nonlinear? As many of our model experiments were done with other forcings as well, we explore their impacts on extracting the solar signal.

[36] Examination of the standard runs can help determine the impact of the overall warming (assumed anthropogenic) on the calculation of solar maximum minus solar minimum changes. Use of historical SST in effect builds in an anthropogenic forcing, since for the time period studied, solar maximum conditions occur later than solar minimum conditions (see Figure 1), and greenhouse gases have been increasing with time, and increasing the SST. One approach, therefore, is to simply drop the last solar maximum and the first solar minimum, and recalculate the temperature response; therefore, instead of using results from 1950 through 2004, the data were analyzed from 1956 through 1998 (hence utilizing 19 years of solar maximum plus minimum data, rather than the original 24 years). The effect on the historical SST themselves is shown in Figure 3 (bottom right). While most of values are unaffected, there is a small reduction in the coverage of warming over the world’s oceans. Shown in Figure 8, bottom two rows, is the

effect on the atmospheric temperature response. Given in Figure 8c is the annual response with the solar cycle as defined originally; in Figure 8d the result with the alternate choice of years. While the troposphere warms in both cases, the response is weakened somewhat when solar minimum comes after solar maximum (seen most clearly in the change divided by the standard deviation, given in Figure 8, right). Since the alternate choice has reduced warming (via the SST) during the (now earlier) solar maximum year, the response independent of this anthropogenic influence on the SST would therefore be in between these two depictions. (Note that dropping 20% of the data randomly does not produce such differences.)

[37] In addition, we make use of the runs that include anthropogenic forcing explicitly. Figures 8a and 8b show the response of the models runs with calculated SST when anthropogenic forcing is included, the original designation of years being shown in Figure 8a and the alternate choice in Figure 8b. The tropospheric response is clearly larger with anthropogenic forcing as expected (Figure 8a), but the stratospheric response has been largely erased, as increasing CO₂ acts to cool the stratosphere.

[38] A second issue concerns the distortion of estimated solar cycle signals by volcanic forcing, because of the approximately 11 years between El Chichon and Mt. Pinatubo. Figure 4c (SV-V) shows results for the simulation with the solar cycle and volcanic influence (using the observed volcanic aerosol record from Sato et al. [1993] updated through 2005). The warming through most of the stratosphere is not affected, which was the direct question. There are some differences from the STANDARD SO-V runs (Figure 4a) in the lower stratosphere, with reduced ozone, negative solar radiation heating rates and cooler temperatures, although the temperature differences between the two experiments are less than 2 standard deviations. Dynamically there are differences as well, with a relative Northern Hemisphere to Southern Hemisphere circulation in the lower stratosphere (not shown) compared with the STANDARD experiment. This result must be viewed with caution given that the volcanic forcing was not allowed to directly affect ozone photochemistry.

3.7. Do the Circulation Changes Match Those Claimed for Solar Forcing?

[39] In general, the changes in dynamics associated with solar forcing are weak, and in the troposphere usually not statistically significant. However, by virtue of the vast number of runs conducted (Tables 1–3), we can investigate whether the simulated patterns are sufficiently consistent to indicate a model response.

[40] As Figure 2b shows, the solar cycle maximum minus minimum results for the standard simulations produced extratropical cooling in the Southern Hemisphere stratosphere during June–August, in contrast with the warming experienced at low latitudes. This increased thermal gradient strengthens west winds (Figure 9), consistent with observations [e.g., van Loon and Shea, 2000]. Not only do the winds increase in the stratosphere in the Southern

Figure 6. Correlation between UV variations (e.g., Figure 1) and (a) temperature, (b) zonal wind, (c) northward EP flux, and (d) vertical EP flux for June–August for the forced (left) east QBO and (right) west QBO.

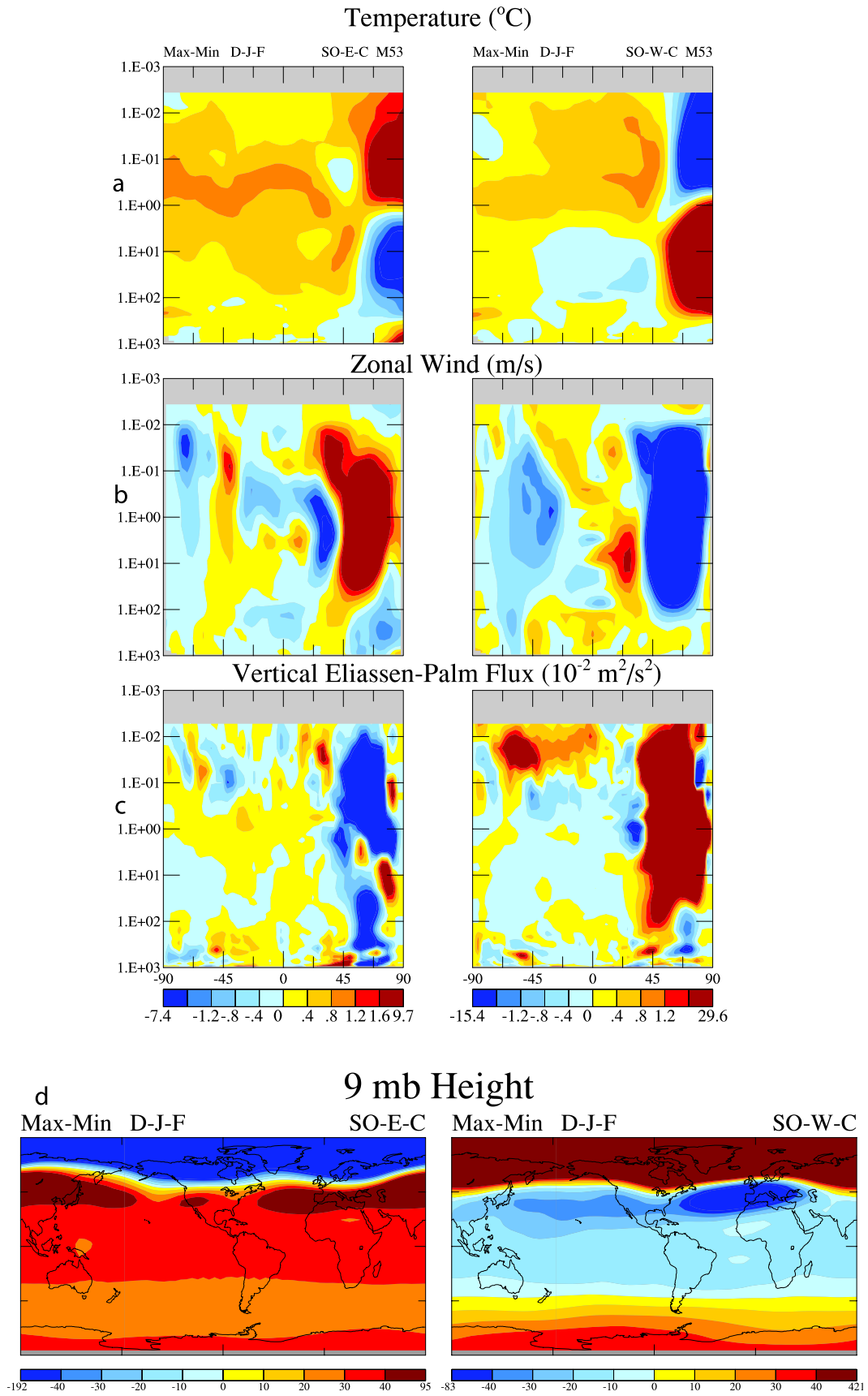


Figure 7. December–February change in (a) temperature, (b) zonal wind, (c) vertical EP flux, and (d) 9 mb height for solar maximum minus solar minimum conditions for the (left) east QBO and (right) west QBO.

Annual Temperature (°C)

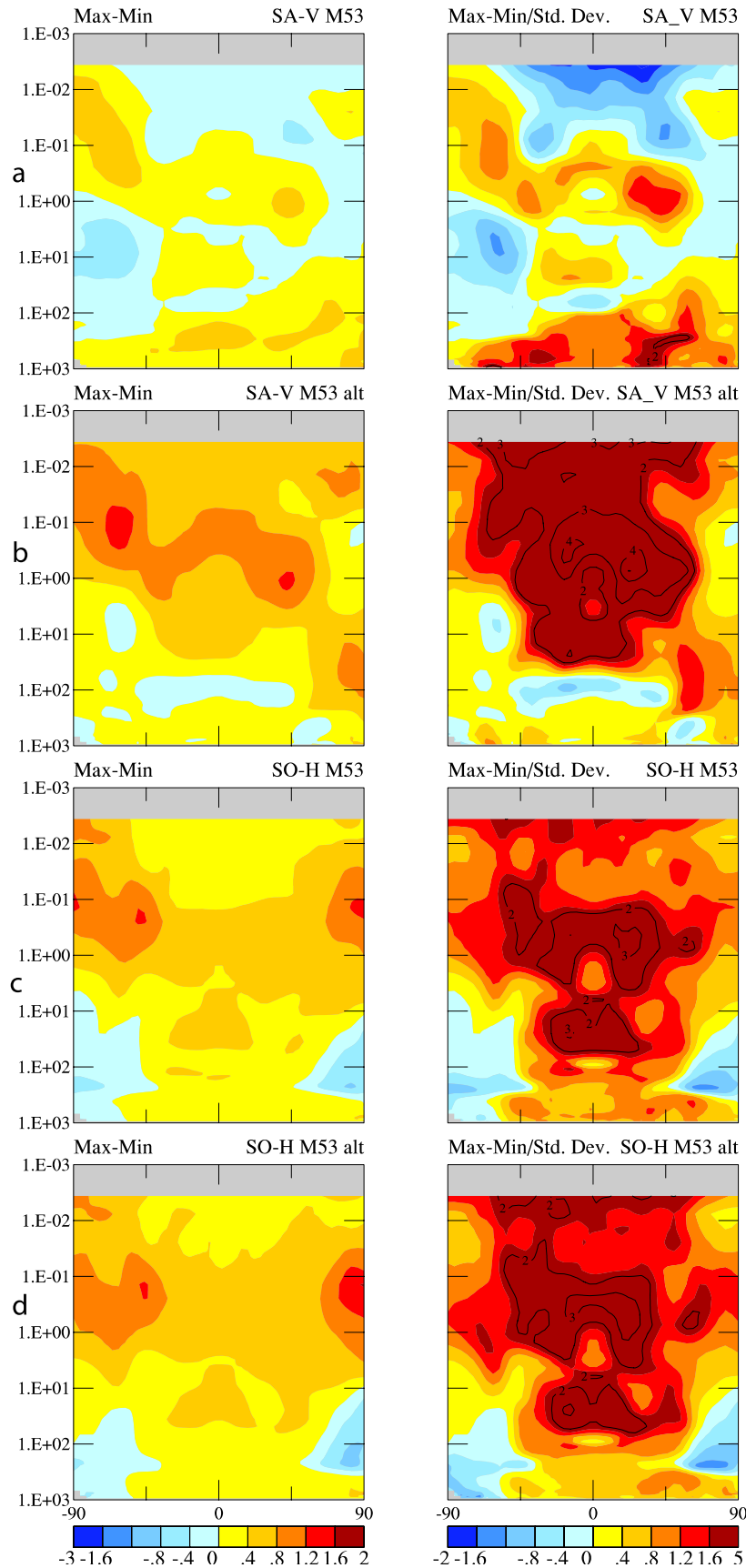


Figure 8

June-July-Aug ZONAL WIND (m/s)

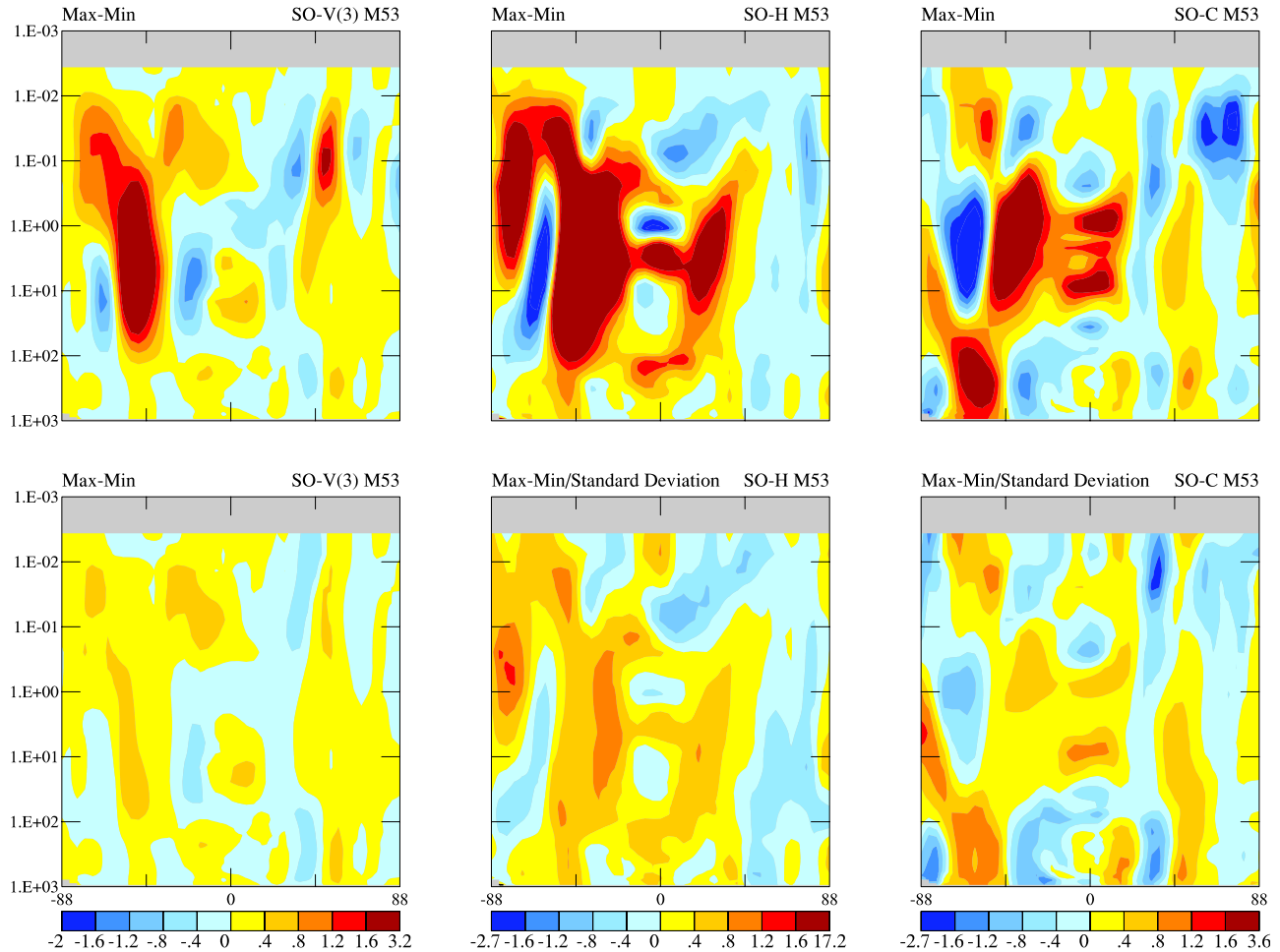


Figure 9. As in Figure 2b except for the change in June–August zonal wind.

Hemisphere extratropics, but the effect extends down to the troposphere, where it is occasionally significant (e.g., SO-C), with magnitudes of a few m/s. This tropospheric component is somewhat weaker with historical SST, and weaker still when SST are calculated, suggesting that a variable tropospheric response has the capacity to minimize the downward propagation of this response. Nevertheless, considering the runs shown in Tables 1–3, of the 26 relevant simulations, all displayed this effect, making the result highly robust, though quantitatively small. The magnitude of the change in the troposphere is large enough to alter sea level pressure fields such that a more positive winter Southern Annual Mode (lower pressure at higher latitudes) is produced in about 70% of the cases (especially with climatological and historical SST). The sea level pressure differences are on the order of -4 mb at high southern latitudes, and $+3$ mb at southern midlatitudes.

[41] As *Kodera and Shibata* [2006] hypothesized, altered planetary wave refraction and an associated relative diver-

gence of the EP flux amplifies the initial tendency for increased west winds arising from the increased temperature gradient produced by the additional heating during solar maximum in the tropics. (The divergence is associated with relative northward wave energy flux, as can be seen in Figure 6 for both QBO phases.) The relative EP flux divergence then leads to a reduction in the stratospheric residual circulation (reduced flow from the summer to winter hemisphere). This effect, as well as the winter zonal wind change descending into the troposphere, is more consistent in the Southern Hemisphere during June–August than in the Northern Hemisphere for December–February, most likely owing to the greater planetary wave forcing and inherent variability during Northern Hemisphere winter (in the real world including QBO effects; as seen in Figure 7, but in observations as well, the effect on the zonal winds in Northern Hemisphere winter is opposite in the two phases). Therefore, on the annual average, the net effect is an increase in the residual circulation from the Southern to

Figure 8. (left) Solar maximum minus minimum annual temperature changes and (right) result divided by the interannual standard deviation with anthropogenic forcing included for (a) calculated SST and (c) historical SST using the UV-defined years in Figure 1. Results when the first solar minimum and last solar maximum years are omitted are shown using (b) calculated SST and (d) historical SST.

Solar Cycle-Stream Function Correlation

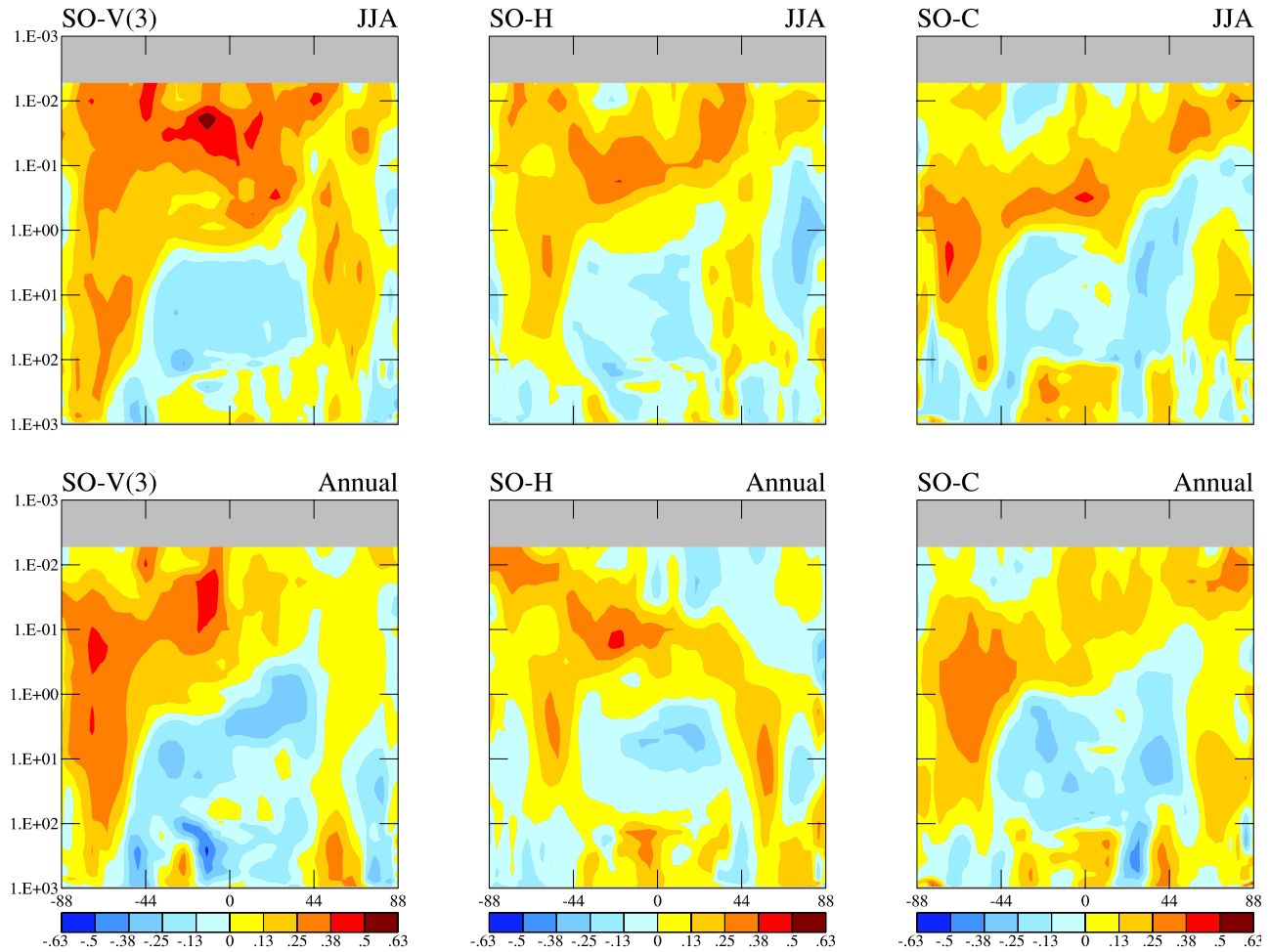


Figure 10. Correlation of the stream function values with solar UV variations, (top) June–August and (bottom) annual average. Negative values indicate a clockwise circulation change in the plane of the panel.

Northern Hemispheres. This is apparent in Figure 10 from the correlation of the varying solar UV irradiance with the stream function value during June–August (Figure 10, top) and annual (Figure 10, bottom) (especially in the stratosphere, the residual stream function change is very similar, as is the difference between solar maximum and solar minimum). Note that in the tropical stratosphere, the UV influence generally accounts for less than 10% of the stream function variance.

[42] To examine the vertical velocity changes associated with the stream function in more detail, we show in Figure 11 the correlation between the June–August (Figure 11, top) and annual UV variations (Figure 11, bottom) with the vertical velocities from the three standard runs. Relative rising air (positive values) can be seen around 50°S in all the cases, extending from the troposphere through the stratosphere. Descent occurs at high southern latitudes, and, in the stratosphere during June–August, in a general region extending from about 40°S to 40°N; however, it is not particularly coherent, and there are differences from run to run. On the annual average, the most consistent descent in the Northern Hemisphere occurs in the extra-

tropics around 45°N, extending down into the troposphere. The annual average descent in the Northern midlatitudes should impact precipitation (see the next section); the simulation of *Shindell et al.* [2006] reported just such a response, and obtained an annual and zonal average precipitation decrease of up to 3%.

[43] *Haigh et al.* [2005] performed a multilinear regression of NCAR/NCEP reanalysis data against measures of various possible “forcings,” including the solar cycle. Their results showed increased zonal winds in the tropics, reduced values in the subtropics, and increases further poleward, which they discussed as a weakening and poleward shift of the subtropical jet stream with a more active sun. A weakening and poleward shift of the subtropical jet stream can be seen in the SO-V and (especially) SO-C runs (Figure 9); the magnitude of the response, peaking at 1 m s^{-1} , is similar to that in the *Haigh et al.* [2005] assessment. The effect in the model is not clearly evident with the historical SST, which contain influences from other phenomena that in the *Haigh et al.* [2005] analysis largely canceled the solar effect when looking at the overall trend; in particular, ENSO variations intensify the subtropical jet. (An additional distinction is

Solar Cycle-Vertical Velocity Correlation

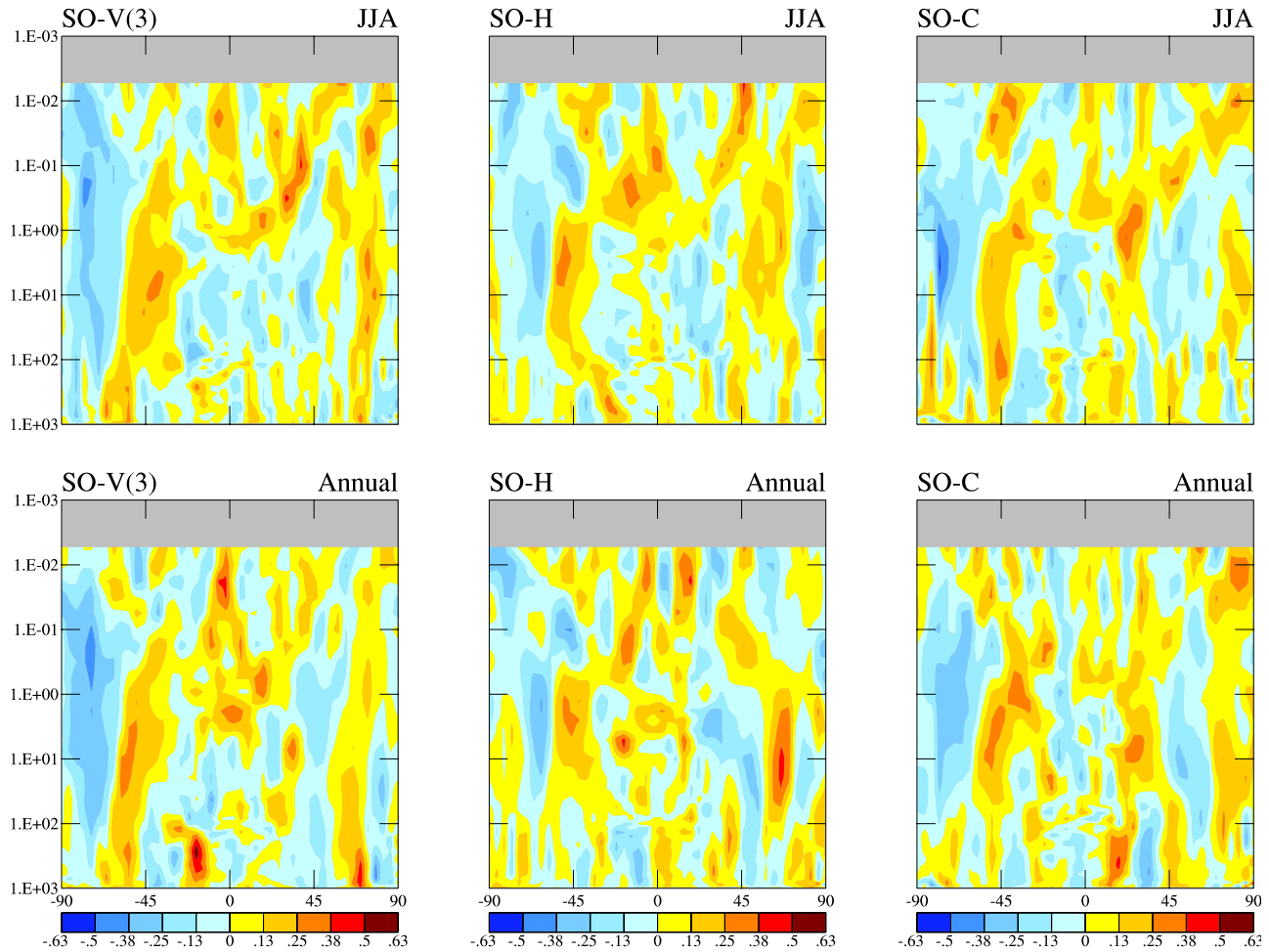


Figure 11. As in Figure 10 but for vertical velocities (positive values indicate upward motion).

that *Haigh et al.* [2005] included all phases of the solar cycle in their analysis, while the results in Figure 9 show solar maximum minus minimum conditions for June–August; the annual average results for solar maximum minus minimum do not show a poleward movement of the subtropical jet either.)

[44] An expansion of the Hadley circulation, associated with this zonal wind change, is evident in the vertical velocity correlation, with added descent in the region $\sim 30\text{--}45^\circ\text{N,S}$ in SO-V and SO-C (Figure 11, bottom). An extension of the Hadley Circulation is a result anticipated in response to warming in the lower stratosphere *Haigh et al.* [2005]. The effect is displaced further poleward with historical SST.

[45] *Kodera and Shibata* [2006] related warming of the tropical lower stratosphere to reduced tropical convection and enhanced off-tropical convection. Since tropical convection drives the December–February Hadley circulation from the Southern to Northern Hemisphere, and off-tropical convection, as occurs in the monsoon region of Southern Asia during June–August, drives the circulation from the Northern to Southern Hemisphere, the latter would be expected to predominate with increased solar heating. The annual average tropospheric circulation change (Figure 10,

bottom) shows an intensification of the circulation from the Northern Hemisphere toward the Southern Hemisphere with climatological and historical SST in the tropics, but, on the three run average, not with calculated values, presumably related to its different SST pattern (Figure 3). Overall this intensification occurred in all 20 of the relevant runs (solar plus ozone change) with climatological or historical SST, and in 2 out of the 6 runs with calculated SST. Treating each run as an independent chance for an increase or decrease, a chi-square test shows that this many occurrences is significant at the 99% level. However, the change is small in magnitude, on the order of a few percent. The vertical velocity correlation (Figure 11) shows a tendency for rising air north of the equator and sinking air just to the south with increased solar UV radiation, which should affect the precipitation, as discussed in the next section.

3.8. Do the Precipitation Changes Match Those Claimed for Solar Forcing?

[46] As with the circulation changes, the observed and modeled precipitation changes are weak, and require multiple experiments to gauge their robustness. The region where the gain in off-equatorial precipitation is expected to be most apparent is in the western Pacific/southeast Asian

June-July-August Precipitation (mm/day)

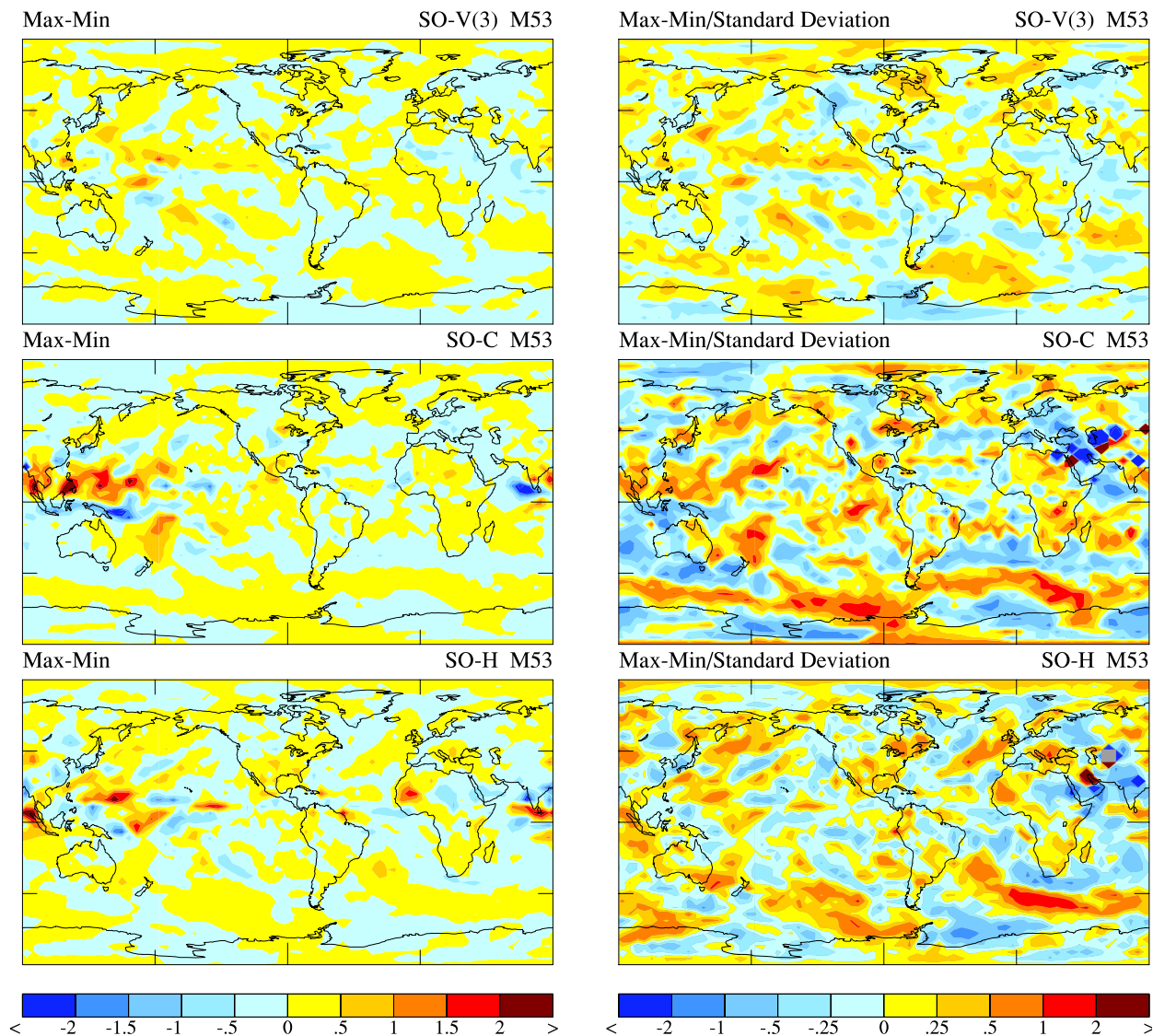


Figure 12. (left) Solar maximum minus minimum change in June–August precipitation and (right) change divided by the standard deviation for the STANDARD experiments: (top to bottom) calculated, climatological, and historical SST.

vicinity owing to the presence of the large landmass. Precipitation changes in the standard experiments during June–August are shown in Figure 12; in all three cases, precipitation increases in this region north of the equator, and decreases in the vicinity of the equator, although again the magnitudes are small. The results for the different resolution experiments with historical and climatological SST all give basically a similar effect (not shown). The localized responses are not necessarily small, being up to 15% of the seasonal mean precipitation. The precipitation increase occurs not only in the western Pacific region, but also at latitudes 10°N – 18°N across the globe. Similarly there is a small precipitation decrease near the equator. This effect is clarified further in Figure 13, giving the percentage of simulations (out of the 26 relevant different runs) which recorded a precipitation increase or decrease at various

latitudes. Results for June–August (Figure 13a, top) and for the annual average (Figure 13a, bottom) are given. During solar maximum conditions, precipitation preferentially shifts north of the equator, with a corresponding decrease to the south; this effect is apparent with both climatological and historical SST (Figure 13b). As was the case for several other tropospheric responses, the simulations with calculated SST produce less consistent changes, although in one of the three simulations it was very similar to the historical value; apparently the ocean-atmosphere interaction can provide additional variability in the model. Note that this response is not affected by the potential anthropogenic warming that is likely inherent in the SST field; when dropping the first minimum and last maximum, the response in SO-H is quite similar to that when using the full data set.

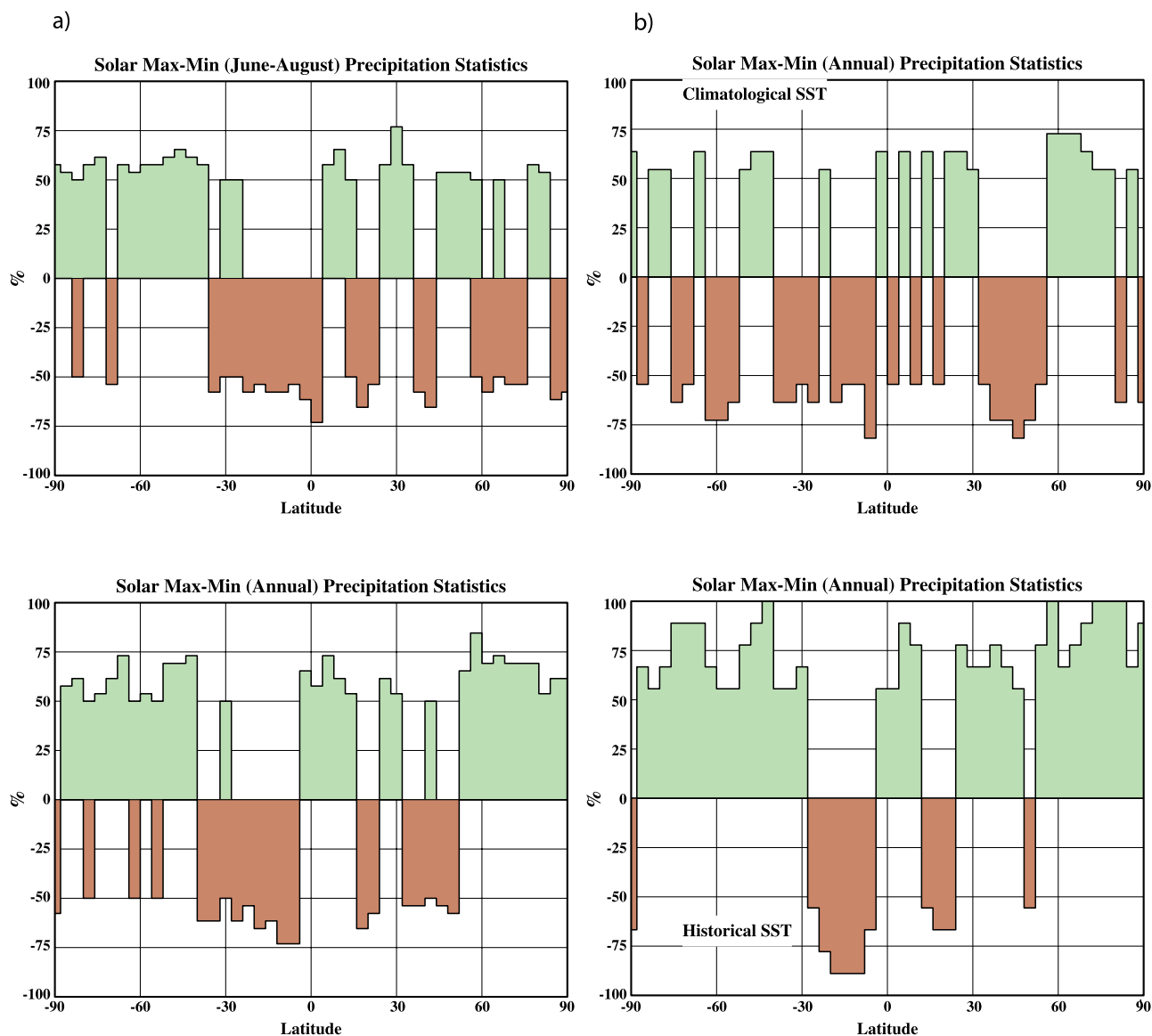


Figure 13. Precipitation statistics for the change in zonally averaged precipitation in the 26 experiments run with both solar forcing and LINOZ or SAGE II ozone changes. (a) (top) June–August and (bottom) annual time periods. (b) Annual average with (top) climatological and (bottom) historical SST.

[47] In addition, on the annual average, especially with climatological SST, reduced precipitation at northern mid-latitudes (at solar maximum) is apparent in the majority of cases, although this is not true with historical SST. These precipitation changes are consistent with the Hadley Cell response discussed above. Note that these precipitation results are presented for solar maximum minus solar min. If one correlates the full solar cycle against the zonal average precipitation, the correlation coefficients are routinely less than 0.1, hence accounting for less than 1% of the zonal average variance.

4. Discussion

[48] We review the model performance with respect to the (often conflicting) observations and other modeling efforts, and for the detected effects, differentiate which of the potential solar forcing mechanisms is likely responsible.

4.1. Stratospheric Response

4.1.1. Upper Stratosphere

[49] As shown in Figure 2a, the general modeled response in the upper tropical stratosphere is a solar maximum minus minimum warming of $\sim 0.7^\circ\text{C}$. The observed changes in reanalysis and rocketsonde data are in the range $1^\circ\text{--}2^\circ\text{C}$ in the tropical upper troposphere [Hood, 2004; Keckhut et al., 2005] although Scaife et al. [2000] report from SSU data values close to those obtained here. Chanin et al. [1998] suggested that as the SSU data are less contaminated by instrument-related errors, they are likely the more accurate. Other modeling efforts have produced stratospheric temperature changes in the range $0.6^\circ\text{--}0.7^\circ\text{C}$ [Tourpali et al., 2003; Austin et al., 2006; Shindell et al., 2006]; or from 0.8° to 1°C [Matthes et al., 2004; Austin et al., 2008]; or as high as $1.1^\circ\text{--}1.3^\circ\text{C}$ [Labitzke et al., 2002; Egorova et al., 2004]. The models' temperature responses are obviously a function of their solar cycle ozone responses, which generally range

from 2% to 3% [Labitzke *et al.*, 2002; Tourpali *et al.*, 2003; Matthes *et al.*, 2004; Egorova *et al.*, 2004; Sekiyama *et al.*, 2006; Shindell *et al.*, 2006; Austin *et al.*, 2006, 2008]. In this study with the LINOZ scheme, peak ozone changes in the tropical stratosphere were close to 2% (Figure 4). Since the dynamical influence is minimal in this region, small differences in the percent ozone change can be important. For example, Matthes *et al.* [2004] used a 3% ozone change calculated from a 2D model of Haigh [1994], which in conjunction with the input UV changes produced a shortwave heating difference of 0.2°K/d; in comparison, with the $\leq 2\%$ ozone change found here, the heating difference was $\leq 0.18^\circ\text{K/d}$, which proportionally translates into the temperature differences of $\sim 0.7^\circ\text{C}$ in these experiments compared to the 1°C warming in theirs.

[50] The importance of the ozone change is further evident in the experiment with the SAGE II solar maximum minus solar minimum ozone change, which peaks at about 4%. With that as the input ozone field, the model produced a temperature change of about 1.4°C (Figure 4e). Given the spread of observations for both ozone and temperature, it is unclear what the precise magnitude of the solar variability effect is in the tropical upper stratosphere. Nevertheless, in all the experiments conducted here with ozone response, the temperature changes in this region are highly significant (Figure 2a).

4.1.2. Midstratosphere

[51] To complicate matters further, this model's peak ozone changes were in the midstratosphere, as is the case with most models. In contrast, satellite data sets indicate the midstratosphere should have minimal, or even negative ozone changes from solar maximum to minimum [Soukharev and Hood, 2006]. Observations of temperature changes in the midstratosphere are somewhat ambiguous, with SSU data indicating warming extending down to 30 km, while reanalysis data indicates little effect in the tropical midstratosphere [see Hood, 2004]. The standard model results show warming down to this level (Figure 2a), although less than at higher altitudes. This is in agreement with the results of the other models discussed above, and is undoubtedly a consequence of their ozone profiles. With the SAGE II ozone change rather than LINOZ photochemistry, the middle stratosphere warming disappears (Figure 4e), presumably because of the reduced ozone in the data set used. Given the uncertainty in the observations, it is again unclear which temperature change result is more accurate. The warming in the standard runs at these altitudes is again significant.

4.1.3. Lower Stratosphere

[52] Reanalysis data in the lower stratosphere suggest some solar-driven warming, although the magnitude and actual location vary among the different studies, ranging from small to substantial, and from tropical to subtropical [Scaife *et al.*, 2000; Hood, 2004; Labitzke *et al.*, 2002; Crooks and Gray, 2005]. Similarly, observations also show a secondary ozone maximum in the lower stratosphere of 2–4% [e.g., Soukharev and Hood, 2006]. The standard model results here all show warming in the lower stratosphere, weaker in magnitude than at higher levels, but still significant (Figure 2a). This warming disappears when ozone photochemistry is invariant (Figure 4b), as does the increased radiative heating, so it is primarily due to radiative

effects (shortwave and longwave) from the photochemically generated ozone change. The standard experiments do have a small ozone maximum in the lower stratosphere (Figure 4), greater with the climatological SST, of 2–3%. Marsh and Garcia [2007] suggested that this was related to anomalies in sea surface temperatures, particularly those associated with ENSO events. In the run with historical SST (hence including ENSO events), the magnitude of the lower stratospheric ozone maximum was intermediate between the climatological and calculated SST; at least in these experiments, it did not seem to be determinant. There is a dynamic influence to the lower stratospheric ozone change at least in the extratropics, where even with invariant ozone photochemistry (but increased solar UV), the altered circulation produced more ozone in the vicinity of the tropopause (Figure 4b).

[53] Warming in this location is weaker with the SAGE II ozone change, even though that change actually featured an increase in ozone in the lower stratosphere; the greater ozone increase in the upper stratosphere helped produce reduced UV heating below, minimizing the effect of lower stratospheric ozone changes (Figure 4d, middle). The large warming noted by Labitzke *et al.* [2002] in reanalysis data ($>1.5^\circ\text{C}$) is not evident in any of these runs, nor was it stronger during the east phase for June–August; the model actually had stronger warming in the tropical lower stratosphere during the west QBO phase in those months (Figure 6). However, the reverse was true in December–February (Figure 7).

[54] Kodera and Kuroda [2002] suggest that the lower stratospheric warming results from reduced upwelling due to weakening of the residual circulation by planetary wave EP flux divergences, and they found the effect to be strongest right in the vicinity of the equator (which then leads to equatorial changes in the troposphere). ERA-40 reanalysis suggests that the warming actually is in the subtropics [Crooks and Gray, 2005]. In the model, the lower stratospheric temperature increase encompasses both the equatorial region and the subtropics (Figure 2a, seen more easily in the bottom panels). The model showed some increased subsidence in response to the solar cycle, especially in June–August (Figure 11, top), although it was not overly consistent among the different simulations, and was not focused on the equator per se. As indicated above, the lower stratospheric warming appears to be more associated with the photochemical ozone change; this is especially true on the annual average, where the warming (Figure 2a) is not associated with any coherent subsidence (Figure 11, bottom). The solar cycle–temperature correlations (Figures 5b–5d) often show a minimal response in the vicinity of the equatorial tropopause, a region where different reanalysis data sets disagree [Labitzke *et al.*, 2002; Crooks and Gray, 2005].

[55] The residual circulation in the Southern Hemisphere does slow somewhat, as implied by the stream function change (Figure 10). Kodera and Kuroda [2002] suggest that the circulation change results from the increased west winds in the stratosphere acting to divert planetary wave energy equatorward, leading to a reduction in wave energy forcing. West wind increases for the winter season do occur (e.g., Figure 9 for June–August), and there is a small increase in EP flux divergence (actually a decrease in the EP flux convergence), peaking at about 10% of control run values in

the upper stratosphere at midlatitudes. And as shown in Figure 6, there is greater equatorward wave energy propagation during June–August (here in both phases of the QBO in the Southern Hemisphere); hence this aspect of the wave-mean flow interaction described by *Kodera and Kuroda* [2002] does occur. But as the results demonstrate, for these model runs the circulation change does not appear to play a major role in the thermal response of the tropical stratosphere; on the annual average, the relative subsidence associated with the circulation change is most consistent at Southern High Latitudes and in Northern midlatitudes (Figure 11, bottom).

4.1.4. SST Influence

[56] As is evident in Figure 2a, the different SST distributions used in these experiments have no discernible influence on the midstratospheric and upper stratospheric response to solar forcing (e.g., temperature response, Figure 2a; wind response, Figure 9; stream function response, Figure 10), while there is some influence in the lower stratosphere (e.g., Figure 5). Some of the details of the dynamic responses differ, but not in a highly significant manner. That is not true for experiments with doubled CO₂ [e.g., *Rind et al.*, 2002] where SST changes play a strong role even in the stratosphere via dynamic influences, probably because in the solar case, the forcing is greatest in the stratosphere and the SST response is small. Therefore, not surprisingly, the stratospheric response to solar forcing is basically driven in situ.

4.2. Tropospheric Response

4.2.1. Temperature

[57] The reports of solar-driven tropospheric warming estimated from observations are somewhat inconsistent among the various studies; in some cases warming encompasses the tropical region while in others it is found away from the tropics, extending from 20 to 60° latitude. The results from the model experiments (e.g., Figures 2a and 5) show weak and generally nonsignificant warming in the troposphere from the equator to 60°N,S when comparing solar maximum and minimum conditions; however, the result is highly robust among the different experiments. The warming is greatest when historical SST are used, similar to those included in reanalysis data from which various researchers have deduced such tropospheric warming. But the result occurs with calculated and climatological SST as well. The magnitude of the modeled warming approaches that determined from NCEP reanalysis data in the midtroposphere when the historical SST are used (about 0.4°C [*van Loon et al.*, 2004]) and is about 1/2 that magnitude when they are calculated or with climatological SST values. *Shindell et al.* [2006] found that increases in tropospheric ozone are necessary to produce the proper magnitude of tropospheric warming. Tropospheric ozone increases do occur in most of these simulations, although not everywhere (e.g., Figures 4 and 5), but the influence is not as big as that resulting from the choice of SST to use.

[58] When correlating the solar cycle with temperature, a positive correlation in the troposphere exists at all model resolutions used with historical SST. It is highly significant, but it only explains about 4% of the variance. With calculated (variable) SST, the correlation is again generally positive, and explains up to 20% of the variance. With

climatological SST, the correlation is mixed; clearly, in these studies, allowing the SST to change does make a difference. (As noted, the effect of historical SST is diminished when the solar minimum year is allowed to come last; averaging the two presentations to provide a relatively unbiased influence shows that the effective tropospheric warming is reduced by some 15% compared with the STANDARD run.)

4.2.2. Precipitation

[59] The primary precipitation changes reported in the literature associated with solar forcing concern reduction of precipitation near and to the south of the equator, with increases off the equator, especially to the north over Southern Asia during solar cycle maximum. Model results do produce this result in general (Figure 12), but as indicated they are generally not highly significant nor do they occur all the time. The results from the compendium of relevant runs (Figure 13) shows that this effect can be seen in 60–70% of the simulations, with localized effects being up to 15% of the seasonal mean precipitation. It is consistent with a Hadley Cell increase during June–August seen for the historical and climatological SST experiments. *Matthes et al.* [2006] also found a tendency for reduced precipitation south of the equator, although in their study it maximized during Northern Hemisphere winter (in the model runs here, that season produces generally similar results to June–August). Another oft reported effect, precipitation reduction at northern midlatitudes, occurs a similar percentage of the time, in this case less often with historical SST. This is consistent with an expansion of the local component of the Hadley Cell and relative subsidence in the affected region (Figure 11).

4.2.3. Circulation

[60] The response of increased west winds (Figure 9) at tropospheric midlatitudes in the Southern Hemisphere (which then results in a tendency for a more positive SAM in the model), is a highly robust result and agrees with the assessment of *Haigh et al.* [2005]. It is a direct result of stratospheric solar forcing, hence less subject to model variability. Zonal wind changes in specific, banded latitudes have been found in different models [e.g., *Larkin et al.*, 2000; *Tourpali et al.*, 2003; *Matthes et al.*, 2004; *Egorova et al.*, 2004] although the magnitudes are weak and the latitudes do not always match those of the observed responses.

[61] The tropospheric circulation response (e.g., poleward shift of the Hadley Cell, and poleward shift and weakening of the jet stream, Figures 9–11) occurs with calculated and climatological SST but not with historical values, probably owing to the other influences inherent in the observed SST variations [*Haigh et al.*, 2005].

[62] Consistent with the precipitation changes, greater subsidence south of the equator does occur in association with increased solar activity (Figure 11).

4.3. Attribution of Solar Forcing Impact on the Troposphere

[63] To address the question raised in the introduction of the cause(s) of the tropospheric response we assume that simulations with climatological SST are primarily driven by stratospheric solar forcing changes, while the other runs have a potential driving component from both SST and stratospheric changes. The strongest temperature response

in the troposphere arises when historical SST and calculated SST are used, which indicates that the SST play a role (at least in the model) in driving the response. The nature of the response with climatological SST though is similar, also indicating warming from solar minimum to solar maximum conditions, with a magnitude about 1/2 to 1/3 that of the other runs. One interpretation is that this indicates the relative importance of stratospheric to surface forcing during the solar cycle. The tropospheric temperature correlation with the complete solar cycle is less widespread and significant when climatological SST are used.

[64] The sea surface temperature response that produces the troposphere warming, at least since 1950, is similar to that described by *White et al.* [1997] of warming in the Pacific and Indian oceans, reproduced in general by the q-flux M53 model. This is more like the response in the model simulations discussed by *Meehl et al.* [2003] of the direct effect of solar heating; it is very different from the La Niña response described from the empirical analysis of *van Loon et al.* [2007].

[65] Precipitation and circulation changes occur in all three SST configurations, so while they may have been influenced by them (note the difference in Figure 12b between the historical and climatological SST results), they do not require them. Somewhat greater SST warming north of the equator in June through August with both historical and calculated values undoubtedly contribute to its effect. Forcing from the stratosphere due to changes in stability as suggested by *Kodera and Shibata* [2006] (among others) is the likely reason for the tropical response of precipitation shifting north of the equator, although in this model the stability change comes primarily from ozone-induced heating of the lower stratosphere, rather than focused stratospheric tropical subsidence. As to why the model disagrees with the *Kodera and Kuroda* [2002] assessment of the importance of tropical subsidence, one obvious possibility is that the model, in all its configurations, has a circulation response that is too broad. However, calculation of the residual circulation (a higher-order quantity) from observations is fraught with difficulty. Also, *Kodera and Kuroda* [2002] acknowledge that “NCEP reanalysis data are poor until the mid-1980s,” and the low-latitude data is not always reasonable.

[66] The precipitation results are more variable when SST are calculated, and the associated tropospheric tropical dynamics differs from that due to solar heating in the historical and climatological SST experiments (actually in one of the three predicted SST experiments it was very similar, while in the other two, it was primarily opposite). It may be that this variability is more representative of the real world, but any such conclusion is tempered since the q-flux-mixed layer model used here does not allow for an ocean dynamical response or involvement of the deep ocean. The latter effect would likely be less important given the timescale of the phenomenon being studied (solar maximum relative to solar minimum, i.e., 5 years); however, if ENSO were to be triggered by subtropical heating, as in the analysis of *van Loon et al.* [2007], the SST generated by the q-flux model would be inappropriate in the tropics. Again, the historical SST analysis performed here (and by *White et al.* [1997]) do not show that response. Nevertheless, it is certainly possible that the Q-flux simulations

produce an inaccurate pattern of response to solar heating, given that it primarily depends on solar radiation received at the surface, and that in turn depends on the modeled cloud cover and its response. As shown in Figure 5 for temperature, the variable SST run actually has the strongest tropospheric correlations with varying UV.

5. Conclusions

[67] In this paper we use a suite of modeling experiments to address a range of aspects of solar cycle forcing of the troposphere/stratosphere system reported in the literature. The results in general show that the stratospheric response is highly repeatable and significant. The tropospheric response is weaker, often not significant, but at times fairly robust among the different simulations for both temperature and precipitation. Warming in the troposphere occurs in most of the simulations, with greater magnitude when historical SST are used (of relevance to reanalysis studies). It generally accounts for < 5% of the interannual variability near the surface (on a zonal average), reaching in some simulations ~15–20% of the variability in the midtroposphere and upper troposphere. However, the warming arises even when climatological SST are used, although it is not as large. These results suggest that both proposed mechanisms for solar influence on the troposphere are operative: dynamical changes in the troposphere due to warming of the lower stratosphere from the solar UV effect on stratospheric ozone; and heating of the surface by increased total solar irradiance, especially in the subtropics.

[68] This effect can be seen in the precipitation response as well. Precipitation tends to decrease south of the equator during solar maximum conditions relative to solar minimum, although the result occurs only 60–70% of the time, and is generally not significant; locally, the effect can account for up to 15% of interannual variability, especially in southern Asia. It appears to be the result of both increased stabilization due to a warmer lower stratosphere, and a sea surface temperature forcing featuring somewhat greater warming north of the equator (with both the historical and calculated SST) during June–August.

[69] The warming in the tropical lower stratosphere arises from increased radiative heating associated with increased lower stratospheric ozone. Subsidence in the tropical stratosphere, the other proposed explanation, is not particularly focused or consistent in the model simulations, especially on the annual average; the effect in June–July may be somewhat more important. The solar UV effect in the stratosphere does produce stronger west winds, altered planetary wave propagation and a change in the residual circulation, with relative subsidence extending over a wide range of latitudes, including the extratropics of the summer hemisphere where it helps reduce tropospheric precipitation.

[70] Zonal west winds generated in the stratosphere under solar maximum (relative to solar minimum) conditions propagate down into the troposphere, especially in the Southern Hemisphere during winter, where they produce a more positive Southern Annual Mode (SAM) in about 70% of the cases. With calculated and climatological SST, the subtropical jet weakens and shifts poleward, along with the Hadley Cell; with historical SST, the poleward shift is less

apparent, most likely owing to other influences affecting the SST.

[71] Other results show that solar cycle effects in combination with the QBO (forced in the model) produce many of the results suggested for them from observations in both solstice seasons, associated with the influence of both horizontal and vertical wind shear on planetary wave propagation. In addition, anthropogenic effects (particularly CO₂ increases) can obscure solar forcing in the stratosphere and influence the derived warming in the troposphere, by virtue of the ordering of solar maximum and solar minimum conditions. Volcanic influences, ~11 years apart for a portion of this time period, can alter the lower stratospheric solar cycle response, although in these runs the volcanic aerosols were not allowed to influence ozone photochemistry, which might produce additional changes. Use of the SAGE II ozone changes rather than the calculated values alters the magnitude of upper stratospheric warming, and the temperature response in the midstratosphere, but produces no obvious changes at lower levels relative to the standard experiments.

[72] There is no systematic influence of model resolution (either vertical or horizontal) on the results of these experiments, which is somewhat surprising since one of the proposed mechanisms for transmitting solar influences down to the troposphere involves synoptic-scale eddies, which are better resolved at the finer resolution. The finer resolution models also have a sharper intertropical convergence zone (ITCZ); and yet the precipitation response to increased solar irradiance, with convection and rainfall moving off the equator, seems similar at all the resolutions used.

[73] There are numerous caveats concerning the results from these models experiments. This model, like many others, is not capable by itself of producing the observed peak ozone response in the upper stratosphere; while utilizing the SAGE II ozone profile change allowed us to estimate some of the effects of this discrepancy, it does not fully indicate what would happen interactively if the model matched observations on its own, including possible influences on the lower stratosphere. Similarly, while the forced QBO helped the model reproduce many features attributed to observed QBO/solar cycle phenomena, the use of a time- (and altitude-) varying QBO could certainly affect some of these conclusions. The use of a coupled atmosphere-ocean model capable of realistically simulating ENSO phenomena would be necessary to assess the solar impact on the tropical Pacific circulation. And a general caveat is that the tropospheric and stratospheric dynamic responses will be affected by the atmospheric background state and the model parameterizations, so would be expected to differ among models.

[74] With these limitations in mind, considered together these modeling experiments seem to verify a relatively robust but modest influence of solar cycle forcing on the troposphere. The climate response in these model runs appears more in the form of “weighting the dice,” rather than having the solar cycle drive a dominant effect; this is true for many other forcing factors (e.g., ENSOs, or volcanic influences on the NAO). Overall, the solar influences appears to be the result of both forcing from above (stratospherically driven) and from below (with an SST influence). Hence many of the contrasting discussions in the literature, from this perspective, all have elements of truth,

but represent only a portion of the complete scenario. In terms of understanding mechanisms, the modeling studies emphasize that various factors can, and generally do, come into play with any forced phenomena in the climate system, and this seems especially true when solar variability is involved [Rind, 2002].

[75] **Acknowledgments.** This work was supported by the NASA Living With A Star program and the NASA Atmospheric Composition focus area. Computer time was provided by the NASA NCCS high-speed computing program. Climate modeling at GISS in general is supported by the NASA Climate Variability and Climate Change focus area.

References

- Austin, J., L. L. Hood, and B. E. Soukharev (2006), Solar cycle variations of stratospheric ozone and temperature in simulations of a coupled chemistry-climate model, *Atmos. Chem. Phys. Discuss.*, *6*, 12,121–12,153.
- Austin, J., et al. (2008), Coupled chemistry climate simulations of the solar cycle in ozone and temperature, *J. Geophys. Res.*, *113*, D11306, doi:10.1029/2007JD009391.
- Balachandran, N. K., and D. Rind (1995), Modeling the effects of UV variability and the QBO on the troposphere/stratosphere system. Part I: The middle atmosphere, *J. Clim.*, *8*, 2058–2079, doi:10.1175/1520-0442(1995)008<2058:MTEOUV>2.0.CO;2.
- Balachandran, N. K., D. Rind, P. Lonergan, and D. T. Shindell (1999), Effects of solar cycle variability on the lower stratosphere and the troposphere, *J. Geophys. Res.*, *104*, 27,321–27,339, doi:10.1029/1999JD900924.
- Bey, I., D. J. Jacob, R. M. Ylantosca, J. A. Logan, B. D. Feld, A. M. Fiore, Q. Li, H. Liu, L. J. Mickley, and M. Schultz (2001), Global modeling of tropospheric chemistry with assimilated meteorology: Model description and evaluation, *J. Geophys. Res.*, *106*, 23,073–23,096, doi:10.1029/2001JD000807.
- Bhattacharya, S., and R. Narasimha (2005), Possible association between Indian monsoon rainfall and solar activity, *Geophys. Res. Lett.*, *32*, L05813, doi:10.1029/2004GL021044.
- Camp, C. D., and K. K. Tung (1997), Surface warming by the solar cycle as revealed by the composite mean difference projection, *Geophys. Res. Lett.*, *34*, L14703, doi:10.1029/2007GL030207.
- Chanin, M. L., V. Ramaswamy, D. J. Gaffen, W. J. Randel, R. B. Rood, and M. Shiotani (1998), Trends in stratospheric temperatures, in *Scientific Assessment of Ozone Depletion: 1998, Global Ozone Research and Monitoring Project, Rep. 44*, p. 5.1–5.59, World Meteorol. Org., Geneva.
- Coughlin, K., and K. K. Tung (2004), Eleven-year solar cycle signal throughout the lower atmosphere, *J. Geophys. Res.*, *109*, D21105, doi:10.1029/2004JD004873.
- Crooks, S. A., and L. J. Gray (2005), Characterization of the 11-year solar signal using a multiple regression analysis of the ERA-40 dataset, *J. Clim.*, *18*, 996–1015, doi:10.1175/JCLI-3308.1.
- Deser, C., and M. L. Blackmon (1993), Surface climate variations over the North Atlantic Ocean during winter: 1900–1989, *J. Clim.*, *6*, 1743–1753, doi:10.1175/1520-0442(1993)006<1743:SCVOTN>2.0.CO;2.
- Egorova, T., E. Rozanov, E. Manzini, M. Haberer, W. Schmutz, V. Zubov, and T. Peter (2004), Chemical and dynamical response to the 11-year variability of the solar irradiance simulated with a chemistry-climate model, *Geophys. Res. Lett.*, *31*, L06119, doi:10.1029/2003GL019294.
- Gleisner, H., and P. Thejll (2003), Patterns of tropospheric response to solar variability, *Geophys. Res. Lett.*, *30*(13), 1711, doi:10.1029/2003GL017129.
- Haigh, J. (1994), The role of stratospheric ozone in modulating the solar radiative forcing of climate, *Nature*, *370*, 544–546, doi:10.1038/370544a0.
- Haigh, J. (2003), The effects of solar variability on the Earth’s climate, *Philos. Trans. R. Soc., Ser. A*, *361*, 95–111.
- Haigh, J., M. Blackburn, and R. Day (2005), The response of tropospheric circulation to perturbations in lower-stratospheric temperature, *J. Clim.*, *18*, 3672–3685, doi:10.1175/JCLI3472.1.
- Hansen, J., G. Russell, D. Rind, P. Stone, A. Lacis, S. Lebedeff, R. Ruedy, and L. Travis (1983), Efficient three-dimensional global models for climate studies: Models I and II, *Mon. Weather Rev.*, *111*, 609–662, doi:10.1175/1520-0493(1983)111<0609:ETDGMF>2.0.CO;2.
- Hansen, J., et al. (2007), Climate simulations for 1880–2003 with GISS model E, *Clim. Dyn.*, *29*, 661–696, doi:10.1007/s00382-007-0255-8.
- Hood, L. L. (2004), Effects of solar variability on the stratosphere, in *Solar Variability and Its Effects on Climate*, *Geophys. Monogr. Ser.*,

- vol. 141, edited by J. M. Pap and P. Fox, pp. 283–304, AGU, Washington, D. C.
- Intergovernmental Panel on Climate Change (2007), *Climate Change 2007: The Physical Science Basis. Contribution of Working Group I to the Fourth Assessment Report of the Intergovernmental Panel on Climate Change*, edited by S. Solomon et al., 996 pp., Cambridge Univ. Press, Cambridge, U.K.
- Keckhut, P., C. Cagnazzo, M.-L. Chanin, C. Claud, and A. Hauchecorne (2005), The 11-year solar-cycle effects on the temperature in the upper-stratosphere and mesosphere: Part I—Assessment of observations, *J. Atmos. Sol. Terr. Phys.*, *67*, 940–947, doi:10.1016/j.jastp.2005.01.008.
- Kodera, K. (2004), Solar influence on the Indian Ocean Monsoon through dynamical processes, *Geophys. Res. Lett.*, *31*, L24209, doi:10.1029/2004GL020928.
- Kodera, K., and Y. Kuroda (2002), Dynamical response to the solar cycle, *J. Geophys. Res.*, *31*(D24), 4749, doi:10.1029/2002JD002224.
- Kodera, K., and K. Shibata (2006), Solar influence on the tropical stratosphere and troposphere in the northern summer, *Geophys. Res. Lett.*, *33*, L19704, doi:10.1029/2006GL026659.
- Kuroda, Y., and K. Kodera (2002), Effect of solar activity on the polar-night jet oscillation in the Northern and Southern Hemisphere winter, *J. Meteorol. Soc. Jpn.*, *80*, 973–984, doi:10.2151/jmsj.80.973.
- Labitzke, K. (1987), Sunspots, the QBO and the stratospheric temperatures in the north polar region, *Geophys. Res. Lett.*, *14*, 535–537, doi:10.1029/GL014i005p00535.
- Labitzke, K. (2004), On the signal of the 11-year sunspot cycle in the stratosphere and its modulation by the quasi-biennial oscillation, *J. Atmos. Sol. Terr. Phys.*, *66*, 1151–1157.
- Labitzke, K., J. Austin, N. Butchart, J. Knight, M. Takahashi, M. Nakamoto, T. Nagashima, J. Haigh, and V. Williams (2002), The global signal of the 11-year solar cycle in the stratosphere: Observations and models, *J. Atmos. Sol. Terr. Phys.*, *64*, 203–210, doi:10.1016/S1364-6826(01)00084-0.
- Lacis, A., and J. E. Hansen (1974), A parameterization for the absorption of solar radiation in the earth's atmosphere, *J. Atmos. Sci.*, *31*, 118–133, doi:10.1175/1520-0469(1974)031<0118:APFTAO>2.0.CO;2.
- Larkin, A., J. D. Haigh, and S. Djavidnia (2000), The effect of solar UV irradiance variations on the Earth's atmosphere, *Space Sci. Rev.*, *94*, 199–214, doi:10.1023/A:1026717307057.
- Latif, M., and T. P. Barnett (1994), Causes of decadal climate variability over the North Pacific and North America, *Science*, *266*, 634–637, doi:10.1126/science.266.5185.634.
- Lean, J., G. Rottman, J. Harder, and G. Kopp (2005), SOLAR contributions to new understanding of global change and solar variability, *Sol. Phys.*, *230*, 27–53, doi:10.1007/s11207-005-1527-2.
- Marsh, D. R., and R. R. Garcia (2007), Attribution of decadal variability in lower-stratospheric tropical ozone, *Geophys. Res. Lett.*, *34*, L21807, doi:10.1029/2007GL030935.
- Matthes, K., U. Langematz, L. L. Gray, K. Kodera, and K. Labitzke (2004), Improved 11-year solar signal in the Freie Universität Berlin Climate Middle Atmosphere model (FUB-CMAM), *J. Geophys. Res.*, *109*, D06101, doi:10.1029/2003JD004012.
- Matthes, K., Y. Kuroda, K. Kodera, and U. Langematz (2006), Transfer of the solar signal from the stratosphere to the troposphere: Northern winter, *J. Geophys. Res.*, *111*, D06108, doi:10.1029/2005JD006283.
- McLinden, C. A., S. C. Olsen, B. Hannegan, O. Wild, M. J. Prather, and J. Sundet (2000), Stratospheric ozone in 3-D models: A simple chemistry and the cross-tropopause flux, *J. Geophys. Res.*, *105*, 14,653–14,666, doi:10.1029/2000JD900124.
- Meehl, G. A., W. M. Washington, T. M. L. Wigley, J. M. Arblaster, and A. Dai (2003), Solar and greenhouse gas forcing and climate response in the twentieth century, *J. Clim.*, *16*, 426–444, doi:10.1175/1520-0442(2003)016<0426:SAGGFA>2.0.CO;2.
- Park, R. J., D. J. Jacob, B. D. Field, R. M. Yantosca, and M. Chin (2004), Natural and transboundary pollution influences on sulfate-nitrate-ammonium aerosols in the United States: Implications for policy, *J. Geophys. Res.*, *109*, D15204, doi:10.1029/2003JD004473.
- Randel, W. J., and F. Wu (2007), A stratospheric ozone profile data set for 1979–2005: Variability, trends, and comparisons with column ozone data, *J. Geophys. Res.*, *112*, D06313, doi:10.1029/2006JD007339.
- Rayner, N. A., D. E. Parker, E. B. Horton, C. K. Folland, L. V. Alexander, D. P. Rowell, E. C. Kent, and A. Kaplan (2003), Global analyses of SST, sea ice and night marine air temperatures since the late nineteenth century, *J. Geophys. Res.*, *108*(D14), 4407, doi:10.1029/2002JD002670.
- Reynolds, R. W., and T. M. Smith (1994), Improved global sea surface temperature analyses, *J. Clim.*, *7*, 929–948, doi:10.1175/1520-0442(1994)007<0929:IGSSTA>2.0.CO;2.
- Rind, D. (2002), The Sun's role in climate variations, *Science*, *296*, 673–678, doi:10.1126/science.1069562.
- Rind, D., and N. K. Balachandran (1995), Modeling the effects of solar variability and the QBO in the troposphere/stratosphere system. Part 2: The troposphere, *J. Clim.*, *8*, 2080–2095, doi:10.1175/1520-0442(1995)008<2080:MTEOUV>2.0.CO;2.
- Rind, D., J. Perlwitz, J. Lerner, C. McLinden, and M. Prather (2002), The sensitivity of tracer transports and stratospheric ozone to sea surface temperature patterns in the doubled CO₂ climate, *J. Geophys. Res.*, *107*(D24), 4800, doi:10.1029/2002JD002483.
- Rind, D., J. Lerner, and J. Zawodny (2005), A complementary analysis for SAGE II data profiles, *Geophys. Res. Lett.*, *32*, L07812, doi:10.1029/2005GL022550.
- Rind, D., J. Lerner, J. Jonas, and C. McLinden (2007), Effects of resolution and model physics on tracer transports in the NASA Goddard Institute for Space Studies general circulation models, *J. Geophys. Res.*, *112*, D09315, doi:10.1029/2006JD007476.
- Sato, M., J. E. Hansen, M. P. McCormick, and J. B. Pollack (1993), Stratospheric aerosol optical depths, 1850–1990, *J. Geophys. Res.*, *98*, 22,987–22,994, doi:10.1029/93JD02553.
- Scaife, A. A., J. Austin, N. Butchart, S. Pawson, M. Keil, J. Nash, and I. N. James (2000), Seasonal and interannual variability of the stratosphere diagnosed from UKMO TOVS analyses, *Q.J.R. Meteorol. Soc.*, *126*, 2585–2604, doi:10.1002/qj.49712656812.
- Sekiyama, T. T., K. Shibata, M. Deushi, K. Kodera, and J. L. Lean (2006), Stratospheric ozone variation induced by the 11-year solar cycle: Recent 22-year simulation using 3-D chemical transport model with reanalysis data, *Geophys. Res. Lett.*, *33*, L17812, doi:10.1029/2006GL026711.
- Shindell, D. T., D. Rind, N. K. Balachandran, J. Lean, and P. Lonergan (1999), Solar cycle variability, ozone and climate, *Science*, *284*, 305–308, doi:10.1126/science.284.5412.305.
- Shindell, D., G. Faluvegi, R. L. Miller, G. A. Schmidt, J. E. Hansen, and S. Sun (2006), Solar and anthropogenic forcing of tropical hydrology, *Geophys. Res. Lett.*, *33*, L24706, doi:10.1029/2006GL027468.
- Smith, T. M., and R. W. Reynolds (2004), Improved extended reconstruction of SST (1854–1997), *J. Clim.*, *17*, 2466–2477, doi:10.1175/1520-0442(2004)017<2466:IEROS>2.0.CO;2.
- Soukharev, B. E., and L. L. Hood (2006), Solar cycle variation of stratospheric ozone: Multiple regression analysis of long-term satellite data sets and comparisons with models, *J. Geophys. Res.*, *111*, D20314, doi:10.1029/2006JD007107.
- Stratospheric Processes and their Role in Climate (1998), SPARC/IOC/GAW assessment of trends in the vertical distribution of ozone, *Rep. 43*, World Meteorol. Org., Geneva.
- Tourpali, K., C. J. E. Schuurmans, R. van Dorland, B. Steil, and C. Bruhl (2003), Stratospheric and tropospheric response to enhanced solar UV radiation: A model study, *Geophys. Res. Lett.*, *30*(5), 1231, doi:10.1029/2002GL016650.
- van Loon, H., and D. J. Shea (1999), A probable signal of the 11-year solar cycle in the troposphere of the Northern Hemisphere, *Geophys. Res. Lett.*, *26*, 2893–2896, doi:10.1029/1999GL900596.
- van Loon, H., and D. J. Shea (2000), The global 11-year solar signal in July August, *Geophys. Res. Lett.*, *27*, 2965–2968, doi:10.1029/2000GL003764.
- van Loon, H., G. A. Meehl, and J. M. Arblaster (2004), A decadal solar effect in the tropics in July August, *J. Atmos. Sol. Terr. Phys.*, *66*, 1767–1778, doi:10.1016/j.jastp.2004.06.003.
- van Loon, H., G. A. Meehl, and D. J. Shea (2007), Coupled air-sea response to solar forcing in the Pacific region during northern winter, *J. Geophys. Res.*, *112*, D02108, doi:10.1029/2006JD007378.
- Wang, Y. M., J. L. Lean, and N. R. Sheeley Jr. (2005), Modeling the Sun's magnetic field and irradiance since 1713, *Astrophys. J.*, *625*, 522–538, doi:10.1086/429689.
- White, W. (2006), Response of tropical global ocean temperature to the Sun's quasi-decadal UV radiative forcing of the stratosphere, *J. Geophys. Res.*, *111*, C09020, doi:10.1029/2004JC002552.
- White, W. B., J. Lean, D. R. Cayan, and M. D. Dettinger (1997), Response of global upper ocean temperature to changing solar irradiance, *J. Geophys. Res.*, *102*, 3255–3266, doi:10.1029/96JC03549.
- White, W. B., M. Dettinger, and D. R. Cayan (2003), Sources of global warming of the upper ocean on decadal period scales, *J. Geophys. Res.*, *108*(C8), 3248, doi:10.1029/2002JC001396.

J. Lean, Naval Research Laboratory, 4555 Overlook Avenue, SW, Washington, D. C. 20375, USA.

A. Leboissitier, J. Lerner, and P. Lonergan, Center for Climate Systems Research, Columbia University, 2880 Broadway, New York, NY 10025, USA.

D. Rind, NASA Goddard Institute for Space Studies, Columbia University, 2880 Broadway, New York, NY 10025, USA. (drind@giss.nasa.gov)